FORMULATION OF BIO-CELLULOSE CONTAINING ALOE GEL EXTRACT FOR ANTI-AGING

SUPHITCHAYA THANITTHEERAPHAN

A Thesis Submitted to the Graduate School of Naresuan University
in Partial Fulfillment of the Requirements
for the Master of Science in Cosmetic Sciences
2021

FORMULATION OF BIO-CELLULOSE CONTAINING ALOE GEL EXTRACT FOR ANTI-AGING

SUPHITCHAYA THANITTHEERAPHAN

A Thesis Submitted to the Graduate School of Naresuan University
in Partial Fulfillment of the Requirements
for the Master of Science in Cosmetic Sciences
2021

Thesis entitled "Formulation of bio-cellulose containing aloe gel extract for anti-aging"

By SUPHITCHAYA THANITTHEERAPHAN

has been approved by the Graduate School as partial fulfillment of the requirements for the Master of Science in Cosmetic Sciences of Naresuan University

Oral Defense Committee

..... Chair
(Assistant Professor Atchariya Yosboonruang, Ph.D.)

..... Advisor
(Professor Jarupa Viyoch, Ph.D.)

..... Internal Examiner
(Associate Professor Tasana Pitaksuteepong, Ph.D.)

Approved

.....
(Associate Professor Krongkarn Chootip, Ph.D.)

Dean of the Graduate School

Title FORMULATION OF BIO-CELLULOSE CONTAINING ALOE GEL EXTRACT FOR ANTI-AGING

Author SUPHITCHAYA THANITTHEERAPHAN

Advisor Professor Jarupa Viyoch, Ph.D.

Academic Paper M.S. Thesis in Cosmetic Sciences, Naresuan University, 2021

Keywords Bio-cellulose, aloe vera, patch, anti-inflammation, anti-aging

ABSTRACT

Photoaging of the skin is caused by ultraviolet exposure that promotes the expression of cytokines such as interleukin 1, epidermal growth factor, and tumor necrosis factor-alpha (TNF-α). Aloe vera has been reported as suppressing the level of TNF-α but aloe vera degrades easily so becomes ineffective against inflammation very quickly. However, applying the dry formulation as a skin patch helps to maintain the stability of the active compound. Bio-cellulose (BC) is a natural material that has a highly porous nanofibril structure that incorporates and releases compounds very quickly. For these reasons, we have an idea to prepare BC containing aloe gel extract and study its anti-inflammatory effect of the extract. An extraction showed that aloe gel extract provided approximately 0.6% of yield. Using high-performance liquid chromatography calculated the aloe-emodin content in the aloe gel extract to be 17.0 ± 3.1 µg/g of lyophilized extract. The cell viability when applying the aloe gel extract to Raw 264.7 cells was studied by colorimetric assay, which showed no cytotoxicity up to 200 µg/mL concentration of aloe gel extract. The anti-inflammatory activity of the aloe gel extract was then evaluated by an enzyme-linked immunosorbent assay at a concentration of 50-200 µg/mL which demonstrated anti-inflammatory activity through the inhibition of TNF-α in LPS-induced Raw 264.7 cells. The BC that was prepared from cultured bacteria *Gluconacetobacter xylinus* was then lyophilized. Dried BC samples were soaked in a solution of formulation that contained the aloe gel extract as well as 0.2% carboxymethyl chitosan and propylene glycol. This

formulation was found to be the most efficient in changing the tensile properties and the appearance of the formulation and increasing the flexibility of the BC. This formulation, designated as Formulation 5, was chosen for stability testing. The results from the stability testing showed that Formulation 5 consisting of aloe gel extract as well as 0.2% carboxymethyl chitosan and propylene glycol provided good stability on physical and mechanical properties during storage. The release study of the aloe gel extract indicated that the release of the aloe-emodin from the BC was time-dependent. These results suggest that the BC containing aloe gel extract has good potential for use in anti-photoaging cosmetic products.

ACKNOWLEDGEMENTS

Firstly, I would to acknowledge for the financial support to this study from the Center of Excellence for Innovation in Chemistry (PERCH-CIC) and facilities support from the Faculty of Pharmaceutical Sciences, Naresuan University.

As for the people who specifically helped with this master's degree thesis, I'm deeply grateful to my thesis advisor Professor Dr. Jarupa Viyoch who made this work possible. Her guidance and support carried me through all the stages of writing my thesis. I cannot thank you enough for helping me.

I would also like to give special thanks to my colleagues of my supervisor. Thanks for all the times they helped me, motivated me, and covered for me. I couldn't have survived without them. They always help and support me with everything as much as they can do.

From the bottom of my heart, I'm indebted to my parents for all their love and support throughout my life. I wholeheartedly appreciate everything you've done for me.

Lastly, I would like to thank Mr. Roy l. Morien and Dr. Kongaphisith Tongpoolsomjit for helping to check the grammar in this thesis.

SUPHITCHAYA THANITTHEERAPHAN

TABLE OF CONTENTS

Page

LIST OF TABLES

Page

LIST OF FIGURES

Page

CHAPTER I

INTRODUCTION

The rationale of study

Skin aging is a regressive process that is associated with skin and the skin support systems (Draelos, 2006). Normally, there are two types of skin aging depending on its cause. Intrinsic aging refers to skin aging caused by internal physiological factors. The other major type is extrinsic aging caused by environmental factors such as ultraviolet (UV) exposure, facial expressions, pollution, sleeping positions, and smoking that lead to premature aging (Sjerobabski-Masnec & Situm, 2010).

Premature aging or photoaging is caused by sunlight exposure depending on the degree of sun exposure and skin pigment. People who live an outdoor lifestyle and are slightly pigmented will increase the higher degree of premature aging (Fisher et al., 2002). UV exposure can induce an enormous effect on the skin depending on the generation of reactive oxygen species (ROS) such as hydroxyl radicals, superoxide, peroxyl, singlet oxygen and hydrogen peroxide (Rinnerthaler, Bischof, Streubel, Trost, & Richter, 2015). Generally, ROS can be destroyed by reacting with other radicals (Silva, Michniak-Kohn, & Leonardi, 2017). Excessive ROS can cause skin aging due to activation of nuclear factor kappa-B inducing the expression of cytokines that stimulate photoaging such as interleukin 1 (IL1), epidermal growth factor (EGF) and tumor necrosis factor alpha (TNF-α) in keratinocytes and dermal cells (Ruland & Mak, 2003; Senftleben & Karin, 2002)

TNF-α is an inflammatory cytokine expressed by various skin cells during extrinsic aging. TNF-α receptors on the cell surface are triggered by UV light, resulting in a decrease in collagen expression and an increase of matrix metallopeptidases (MMPs) expression. These factors contribute to the degradation of the extracellular matrix (ECM) which comprises collagen fibrils as a primary component that gives the strength of the skin (Choi, Lee, & Park, 2017).

The strategies to prevent photoaging include prevention of UV penetration into skin by using physical and chemical sunscreens, scavenging or quenching of ROS by antioxidants, and prevention or decreasing of inflammation using anti-inflammatory compounds (Pillai, Oresajo, & Hayward, 2005).

Aloe vera is one of the medical plants vastly used in biomedical because of its biological properties (Surjushe, Vasani, & Saple, 2008). It comprises many active compounds such as water-soluble minerals, vitamins, polysaccharides, organic acids, enzymes and phenolic compounds (Maan et al., 2018). A previous study discovered that aloe gel containing glucomannan interacts with growth factor receptors on the fibroblast via proliferation activity. It enlarges collagen synthesis after administering aloe vera topical and oral routes (Chithra, Sajithlal, & Chandrakasan, 1998). Other studies represented the anti-inflammatory activity of aloe-emodin in murine macrophages. The results showed that aloe-emodin inhibited nitric oxide production, suppressed the level of cyclooxygenase-2 (COX-2), prostaglandin E2 (PGE2) production (Park, Kwon, & Sung, 2009), and TNF-α production (Harhaji et al., 2007).

However, the formulation design is important for increasing the stability of the active ingredient for anti-inflammatory activity. Patch, a dry formulation that can maintain the stability of the active compound, is one of the dosage forms that appeal to our attention. (Cherukuri, Kiranmai, Cherukuri, & Ganapuram, 2017). In addition, it generally enhances the transport of active compounds by altering the skin barrier functions through increasing hydration of the stratum corneum (Suksaeree, Monton, Charoenchai, & Pathompak, 2014).

Nowadays, bacterial cellulose or bio-cellulose (BC) has become famous due to it having unique properties including high purity, high mechanical strength and non-toxic (Halib, Mohd Amin, & Ahmad, 2012; Perugini, Bleve, Cortinovis, & Colpani, 2018). BC has the ability to hold water with a high amount because of its porous nanofibril structure. For these reasons, we have an idea to prepare bio-cellulose containing aloe gel extract and study its anti-inflammatory effect of the extract which could be expected to use as an anti-photoaging product in the future.

Objectives of the study

1. Major: To prepare bio-cellulose containing aloe gel extract.
2. Minor: To evaluate the physical and mechanical properties of bio-cellulose containing aloe gel extract.
3. Minor: To determine the release of the marker.

Expected output of the study

Bio-cellulose containing aloe gel extract from this study has an anti-inflammatory effect and could be used as an anti-photoaging product in the future.

Scope of research

In the present study, preparation of the aloe gel extracts and bio-cellulose were performed. In addition, high-performance liquid chromatography was used to determine an aloe-emodin in the extract. The extract was studied on murine macrophage to confirm an anti-inflammatory activity. After that, aloe gel extract was immersed with the bio-cellulose, dried to keep in dry form and studied on stability testing. The physical and mechanical properties of BC were then evaluated. Finally, the release of the marker was determined.

CHAPTER II

LITERATURE REVIEW

Skin structure

Skin is the largest organ in our body and covers our body for protecting bone and tissues. The skin comprises three layers including epidermis, dermis and subcutaneous. The structure of the skin is shown in Figure 1.

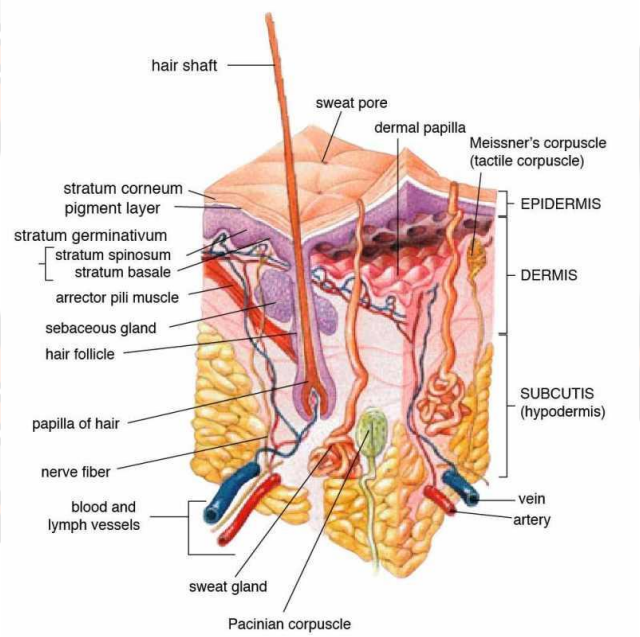

Figure 1 Structure of the skin

Source: https://www.ncbi.nlm.nih.gov/books/NBK470464/#article-21212.s13

1. Epidermis layer

The epidermis layer includes the stratum basale, stratum spinosum, stratum granulosum, stratum lucidum and stratum corneum as shown in Figure 2

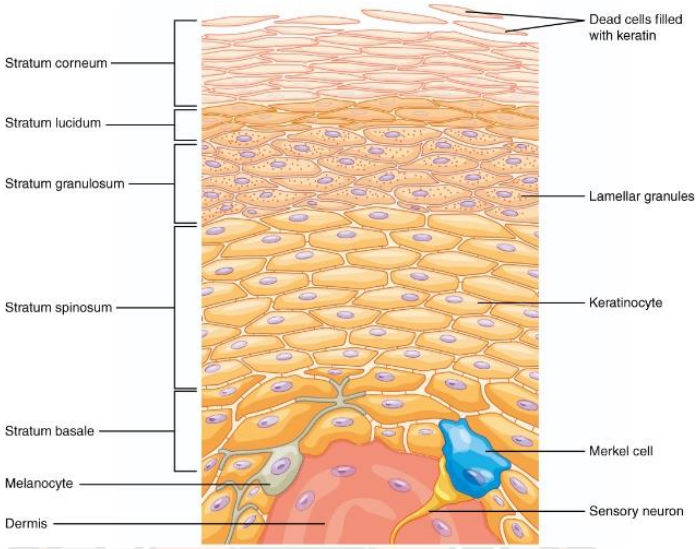

Figure 2 Layers of the epidermis

Source: https://opentextbc.ca/anatomyandphysiology/chapter/5-1-layers-of-the-skin/

1.1 Stratum basale

This layer is considered to be the last layer of the epidermis, which is separated from the dermis by the basement membrane and appended basement membrane by hemidesmosomes. A basal cell is a cuboidal-shaped stem cell that produces the keratinocytes. Another important cell in this layer is melanocytes. Melanocytes produce melanin pigment that is hair and skin color (Yousef, Alhajj, & Sharma, 2021).

1.2 Stratum spinosum

This layer consists of 8-10 cell layers of keratinocytes. They are also known as prickle cells. This layer consists of dendritic cells called Langerhans cells. Langerhans cell is a network of the immune system (Yousef et al., 2021).

1.3 Stratum granulosum

This layer consists of 3-5 cell layers of keratinocytes. Stratum granulosum has diamond-shaped cells with keratohyalin granules and lamellar granules. Keratohyalin granules are proteins that are found in granules and may be involved in the formation of keratin. The lamellar granules contain glycolipids and act as glue to help cells stick together (Yousef et al., 2021).

1.4 Stratum lucidum

This layer consists of 2-3 cell layers of keratinocytes. This layer is the smooth and translucent layer that is found only in the thick skin of the palms, soles and digits (Yousef et al., 2021).

1.5 Stratum corneum

This layer contains 20-30 cell layers of keratinocytes. The stratum corneum is the upper layer that is in contact with the environment. It contains corneocytes that are dead cells which are periodically shed and replaced by cells that are pushed up by the stratum granulosum. The main function of the stratum corneum is to act as the primary barrier between the body and the environment (Yousef et al., 2021).

2. Dermis layer

The dermis consists of two layers; the papillary and reticular layers, as shown in Figure 3.

2.1 Papillary layer

This layer is the upper layer. This layer contains cellular components including fibroblasts, mast cells, macrophages and dermal dendrocytes. The ECM of the papillary layer consists of a network of thin collagen and elastic fibers. Most are the location of the capillaries that feed the epidermis (Kawasumi, Sagawa, Hayashi, Yokoyama, & Tamura, 2012).

2.2 Reticular layer

This layer is the lower layer. This layer is thicker than the papillary layer and is characterized by ECM containing a network of coarse collagen and elastic fibers. Elastin fibers provide elasticity to the skin and collagen fibers provide structure and tensile strength (Kawasumi et al., 2012).

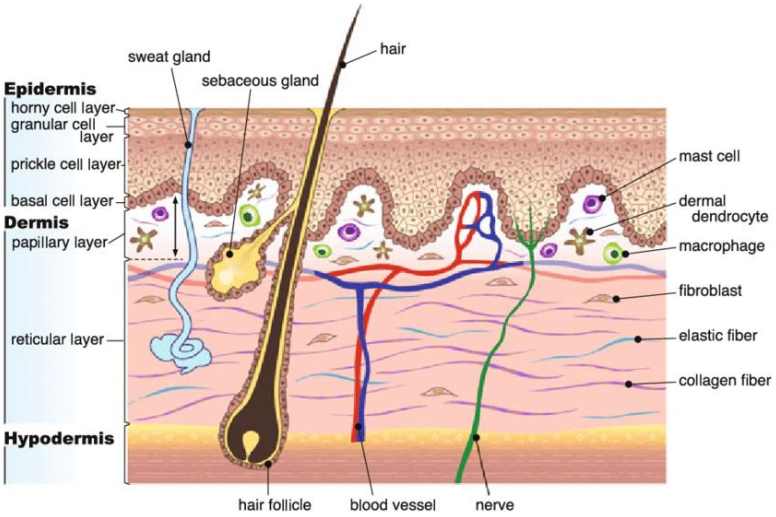

Figure 3 Layers of the dermis

Source: https://www.researchgate.net/figure/Adult-human-skin-is-a-layered-organ-consisting-of-an-epidermis-and-a-dermis-The_fig1_233976352

3. Subcutaneous layer

It is the deepest layer of skin and consists of adipose tissue. Hair follicles, sensory neurons and blood vessels were found in this layer (Kawasumi et al., 2012).

Skin aging

Skin aging is a decadent process that relates to skin and the skin support systems including the bones, cartilages, and subcutaneous compartments (Draelos, 2006). Generally, there are two types of skin aging. Skin aging caused by internal physiological factors is called intrinsic aging. The other type major type is known as extrinsic aging and is caused by environmental factors such as sunlight exposure, smoking, pollution, facial expressions, and sleeping positions (Farage, Miller, Elsner, & Maibach, 2008; Sjerobabski-Masnec & Situm, 2010).

1. Intrinsic aging

Intrinsic aging is also known as aging because of time. Within the skin, collagen synthesis slows down and elastin has decreased. Dead skin cells do not quickly shed and slightly decrease new skin cells. The signs of intrinsic aging are fine wrinkles, thin and transparent skin due to loss of underlying fat, bones shrinking away from the skin due to bone loss which causes sagging skin, dry skin, disability to sweat sufficiently resulting in cool skin, graying hair, hair loss and unwanted hair (Fisher, 2005).

2. Extrinsic aging

Skin aging by external factors often acts together with normal skin aging. External factors cause premature skin such as facial expressions, sunlight, gravity, sleeping positions and smoking. However, the two biggest exogenous factors that affect the skin are smoking and exposure to UV light (Kennedy et al., 2003).

Smoking causes skin damage because it decreases capillary blood flow to the skin. As a result of produces oxygen and nutrient degradation in cutaneous tissues. It has been shown that those who smoke have less collagen and elastin fibers in the dermis. It causes the skin to become slack, hardened and less elastic. Smoke causes damage to collagen and elastin in lung tissue and may occur in the skin as well (Leow & Maibach, 1998).

More than 90% of visible skin aging is caused by the effects of sunlight (Südel et al., 2005). UV also makes damage to the genetic material. Ultraviolet B forms pyrimidine dimers that finally result in mutation through errors in DNA replication. Ultraviolet A radiation makes genetic damage through the production of ROS or free radicals. Free radicals can also destroy numerous cellular processes such as the upregulation of matrix metalloproteinases (Goukassian & Gilchrest, 2004).

Molecular mechanisms in skin aging

1. Oxidative Stress

ROS play a role in dermal extracellular matrix modification of both intrinsic aging and photoaging. ROS can be produced from different sources including the mitochondrial electron transport chain, peroxisomal and endoplasmic reticulum

localized proteins, the Fenton reaction, and enzymes such as cyclooxygenases, lipoxygenases, xanthine oxidases and nicotinamide adenine dinucleotide phosphate (NADPH) oxidase (Rinnerthaler et al., 2015). Under UV radiation, cellular chromophores absorb the energy and get an excited result that produces oxidation products and ROS. ROS inhibit the action of receptor protein tyrosine phosphatases (RPTPs) by binding with cysteine in the catalytic sites of RPTPs (Rittié & Fisher, 2015), promoting the level of phosphorylated receptor tyrosine kinases (RTKs) and inducing downstream signaling pathways including the stimulation of mitogen-activated protein kinase (MAPK) and subsequent nuclear factor-κB (NF-κB) and transcription factor activator protein-1 (AP-1). Activated NF-κB and AP-1 inhibit collagen production and increase MMPs, resulting in the decrease of collagen content in aging skin (Kammeyer & Luiten, 2015).

2. Inflammation

UV radiation stimulates the formation of ROS which activates NF-κB. The activation of this transcription factor increases the expression of proinflammatory cytokines and growth factors such as IL-1, TNF-α and EGF. These cytokines signal to the MAPK pathway to activate AP-1. The transcription factor AP-1 is formed from the heterodimerization of transcription factor precursors c-Fos and c-Jun. This increases the effects of MMPs which lead to collagen degradation and procollagen inhibition (Poon, Kang, & Chien, 2015).

TNF-α and skin aging

Normally, the cause of inflammation in two types of skin aging such as intrinsic and extrinsic aging is the generation of ROS. There are three main signaling pathways stimulated by UV and ROS which are responsible for the activation of many inflammatory genes and genes implicated in skin aging. These pathways such as MAP kinase pathway, NF-κB pathway, and nuclear factor of activated T-cells (NFAT) pathway. There are many interrelate between the pathways in terms of controlling gene activity. UV, ROS, or a specific cytokine such as TNF-α, or IL-1, may activate more than one pathway to increase the inflammatory activity. The cytokines, chemokines, and hormones generated and secreted from keratinocyte and

fibroblast cells after UV exposure, after that enhance skin aging and inflammation by binding to their specific receptors on adjoining cells in the skin. This binding activates signaling pathways that lead to the generation of inflammatory mediators. In addition, cytokines such as IL-1, TNF-α, and PGE-2, can bind and activate receptors on the same cells. Finally, cytokines such as TNF-α, IL-1, and PGE-2 can up-regulate the synthesis of their receptors, thereby further enhancing the inflammatory response, thus increasing the destruction effects on the skin (Fuller, 2019).

Previous studies showed that TNF-α plays a crucial role in the early process of inflammation (Bruunsgaard, Skinhøj, Pedersen, Schroll, & Pedersen, 2000; Ritsu et al., 2017). Moreover, the pro-inflammatory cytokine TNF-α inhibits collagen synthesis and enhances collagen degradation by increasing the production of MMPs.

Aloe vera

Aloe vera (scientific name *Aloe barbadensis* Miller) is classified in the Asphodelaceae (Liliaceae) family. It is mostly found in dry regions such as Africa, Asia, Europe and America (Maan et al., 2018).

Aloe vera is a succulent, soft plant containing a high-water content of about 99 - 99.5%. The solid contents in aloe vera are 0.5–1% of the gel and are composed of a variety of active components such as fat and water-soluble minerals, simple/complex polysaccharides, vitamins, enzymes, organic acids, and phenolic compounds. The leaf of aloe vera composed of three layers such as gel, rind, and latex. Table 1 summarizes the various compounds present in aloe vera gel (Hamman, 2008).

Table 1 Summary of various compounds present in aloe vera gel

Class	Compounds
Amino Acid	Alanine, arginine, aspartic acid, cysteine, glutamic acid, glycine, histidine, hydroxyproline, isoleucine, leucine, lysine, methionine, phenylalanine, proline, threonine, serine, tyrosine and valine

Anthraquinone	Aloe-emodin, aloetic acid, anthranol, aloin A & B, anthracine, anthranon, barbaloin, chrysophanic acid, emodin, ethereal oil, ester of cinnemonic acid, isobarbaloin, and resistannol
Carbohydrates	Lignins and sugars such as arabinose, cellulose, fructose, fucose, galactose, glucose lactose, maltose, mannose, pectic substance, rhamnose, sucrose, uronic acids and xylose
Chromones	8-C-glucosyl-(2′-O-cinnamoyl)-7-O-methylaloediol A, 8-C-glucosyl-(S)- aloesol, 8-Cglucosyl-7-O-methyl-(S)-aloesol, 8-C-glucosyl-7-O-methylaloediol, 8-C-glucosylnoreugenin, isoaloeresin D, isorabaichromone and neoaloesin A
Dietary Fibers Enzymes	Alkaline phosphotase, amylase, carboxypeptidase, catalase, cellulase, cyclooxidase, cyclooxygenase, lipase, oxidase, peroxidase, phosphoenolpyruvate carboxylase and superoxide dismutase
Hormones	Auxins and gibberllins
Inorganic Compounds	Minerals such as calcium, chlorine, chromium, copper, iron, magnesium, manganese, phosphorous, potassium, sodium and zinc
Miscellaneous including organic compounds and lipids	Arachidonic acid, γ-linolenic acid, triglicerides, triterpenoid, potassium sorbate, salicylic acid and uric acid
Organic Acids	Acetic acid, citric acid, formic acid, fumaric acid, lactic acid, malic acid, pyruvate, succinic acid and tartaric acid
Proteins	Lectins and lectin-like substance
Sterols	Cholesterol, campesterol, lupeol and beta sitosterol
Vitamins	Vitamin A, C, E, B1, B2, B6, B9 and choline

Source: Hamman, 2008

Various forms of aloe vera are used in a variety of products such as aloe vera juice, concentrate and powder (Hamman, 2008). Some of its effects in pharmaceuticals and cosmetics are summarized in Table 2 and Figure 4.

Table 2 Pharmacological activities of aloe vera components

Component	Effect
Glycoproteins	Wound healing, cell proliferation, anti-allergy
Mannos-6-phosphate	Wound healing, anti-inflammation
Barbaloin	Purgative
Aloe-emodin, emodin	Purgative, cell proliferation, anti-cancer, antiprotozoal, antibacterial, anti-oxidant, Anti-inflammation
Polysaccharide	Anti-cancer, anti-inflammation
Acemannan	Immunomodulation, anti-microbial, anti-tumor
β-sitosterol	Anti-inflammation, angiogenesis

Source: Hamman, 2008; Harhaji et al., 2007; Park et al., 2009

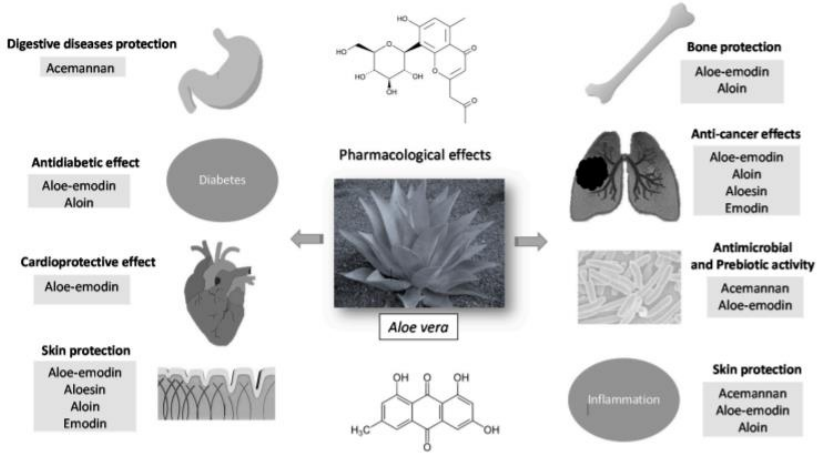

Figure 4 Pharmacological activities of the main components of aloe vera

Source: Sánchez, González-Burgos, Iglesias, & Gómez-Serranillos, 2020

Some effects of aloe vera that are demonstrated with pharmaceutical and cosmetics.

1. Healing effect

In *in vitro* studies, aloe vera significantly stimulated cell proliferation and the migration of fibroblasts and keratinocytes cells (Teplicki et al., 2018). For *in vivo* studies, the common model used when studying animals, topical aloe vera promoted healing of dermal incisions by decreasing the number of inflammatory cells (Brandão, Araújo, Araújo, Santos, & Miguel, 2016).

2. Antioxidant property

Antioxidants are compounds that slow down or inhibit biomolecule oxidative damage because of ROS. The antioxidant activity of aloe vera in this study was showed that anthraquinones and related compounds at concentration 10 µM possess peroxyl radical scavenging activity (Sun et al., 2017).

3. Antimicrobial activity

Different methods have been used to evaluate the antimicrobial activity of aloe vera and its main components. One of the substances attributed to antibacterial activity against *Staphylococcus aureus* is aloe-emodin which performs by blocking biofilm generation and extracellular protein creation (Xiang et al., 2017). In the case of *Pseudomonas aeruginosa*, aloe vera extracts have been shown to inhibit the growth of multidrug-resistant *Pseudomonas aeruginosa* at MIC_{50} and MIC_{90} values of 200 µg/mL (Goudarzi, Fazeli, Azad, Seyedjavadi, & Mousavi, 2015). Aloe vera inner gel also restrained other gram-negative bacteria (*Helicobacter pylori* and *Escherichia coli*) as well as the fungus *Candida albicans* (Cataldi et al., 2015).

Antiviral activity of aloe vera has been examined for herpes simplex virus type 1 and H1N1 subtype influenza virus. Aloe vera extract gel at concentrations of 0.2% to 5% showed antiviral activity against herpes simplex virus type 1 on Vero cells by inhibiting its growth (Rezazadeh, Moshaverinia, Motamedifar, & Alyaseri, 2016).

4. Anti-inflammatory effect

Most studies on the anti-inflammatory activity of aloe vera extract were examined in murine macrophage Raw 264.7 cells. The potential of anti-inflammatory activities depends on the inhibition effect of cytokines. Aloe-emodin showed inhibited nitric oxide production, suppressed the level of COX-2, PGE2 production (Park et al., 2009), and TNF-α production (Harhaji et al., 2007). Moreover, inflammatory cytokines are related to the aging process. The decrease of inflammatory cytokines resulted in a decrease of MMPs and the prevention of skin aging.

Aloe-emodin

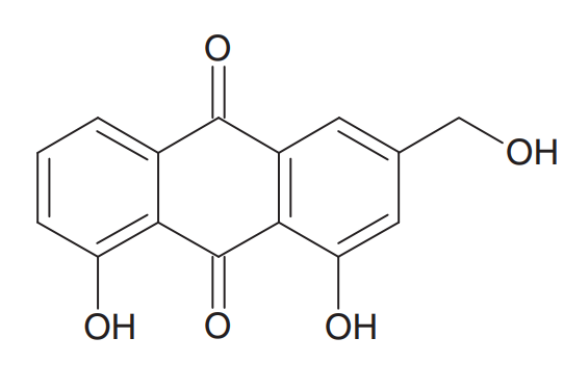

Figure 5 Chemical structure of aloe-emodin

Source: Mandrioli, Mercolini, Ferranti, Fanali, & Raggi, 2011

Aloe-emodin is an anthraquinone as shown in Figure 5 and found in the gel, sap or leaves of aloe vera. Aloe-emodin has been reported for anti-inflammatory effect in many studies as described above. The chemical properties of aloe-emodin were described below.

Molecular Formula	:	$C_{15}H_{10}O_5$
Molecular Weight	:	270.24 g/mol
Melting Point	:	223.5°C
Log P	:	3.254
Solubility	:	DMSO, 3 mg/mL at 25 °C

The forced degradation data of aloe emodin is shown in Table 3. That data indicates that aloe emodin is more sensitive to acid (29.22%) and water degradation (36.23%), moderate to oxidation degradation (61.87%) and has fewer effects under daylight (85.74%) and dry heat degradation (89.23%) (Narayanan, Jadhav, & Kadam, 2015). Hence, the design formulation and packaging are important. This information may help to prevent degradation during storage. Avoidance of acidic conditions and moisture may increase the stability of aloe-emodin in the formulation.

Table 3 Forced degradation data of aloe-emodin

Exposure conditions	**Time (h)**	**Recovery (%) aloe emodin**
Acid (0.1 N HCl) reflux at 80°C	2	29.22
Base (0.1 N NaOH) reflux at 80°C	2	81.93
H_2O_2, (6% v/v)	3	61.87
Dry heat (105°C)	8	89.23
Water, reflux at 80°C	8	36.23
Photostability-day light	8	85.74

Source: Narayanan et al., 2015

Bio-cellulose

The first report involving the production of cellulose from bacteria sources was produced in 1886. The author of that report examined the biosynthesis of cellulose by *Acetobacter xylinum*, an acetic acid bacterium that secrets a plentiful three-dimensional network of cellulose fibrils under aerobic conditions using glucose as a carbon source. The *Acetobacter xylinum* is the most efficient and investigated producer being reclassified afterwards within the genus *Gluconacetobacter xylinus* as *G. xylinus* (Esa, Tasirin, & Rahman, 2014).

Bio-cellulose exists as a basic structure of fibril that consists of β-1→4 glucan chain with molecular formula $(C_6H_{10}O_5)n$. The glucan chains are grasped together by both inter- and intra-hydrogen bonding (Figure 6). Microfibrils of BC approximately 100 times smaller than plant cellulose (Ruka, Simon, & Dean, 2012) were first reported in 1949.

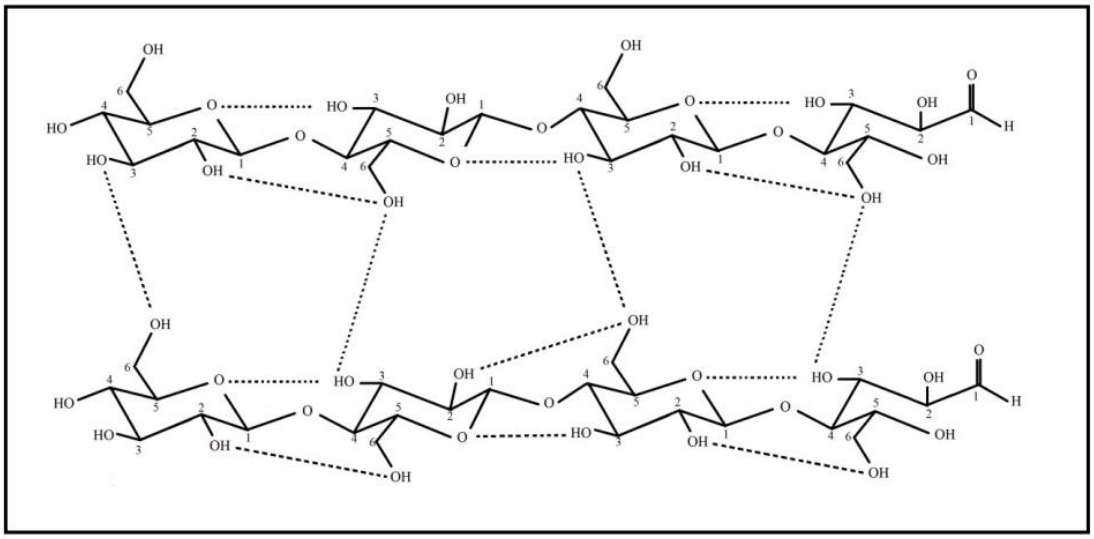

Figure 6 Inter- and intra-hydrogen bonding of bio-cellulose

Source: Esa et al., 2014

Factors that affect *Gluconacetobacter xylinus* growth (Siti et al., 2014)

1. Carbon Sources

Carbon sources contain carbohydrates which are compounds belonging to the monosaccharides and disaccharides. It is related to the fermentation of bio-cellulose (BC). The structure of BC is produced from glucose, sucrose and lactose so the addition of sucrose should be appropriate. However, excess addition of sucrose can cause new residual waste. Alternatively, the addition of too little sucrose results in the inefficient production of BC.

2. Nitrogen Source

Nitrogen sources can be applied in organic or inorganic compounds. Yeast extract and casein are good choices used for the growth and formation of *Gluconacetobacter xylinus*.

3. pH

Although *Gluconacetobacter xylinus* can grow well at a pH between 3.5-7.5, pH 4.3 is the most suitable for the production of BC. Under alkaline conditions, the cell metabolism of these bacteria will be disturbed.

4. Temperature

The suitable temperature for the growth of bacteria *Gluconacetobacter xylinus* is 28°C-31°C which is typically room temperature. A temperature of more than 31°C can cause damage in *Gluconacetobacter xylinus* and can lead to bacteria death.

5. Oxygen

Gluconacetobacter xylinus are aerobic bacterium. This bacterium needs oxygen in its process of growth, development and activity. When lack of oxygen, these bacteria will encounter an interruption in growth which can lead to death.

Some applications of bio-cellulose

1. Facial mask

Bio-cellulose was prepared and incorporated with cosmetic ingredients. BC can hold a high amount of water because BC has a highly porous nanofibril structure. These results make BC incorporate and release compounds very quickly (Pacheco et al., 2018).

2. Wound dressing

Bio-cellulose was prepared by immersing BC with chitosan. The Results showed that BC and BC-chitosan (Ch) membranes sustained appropriate moisture. The effects of BC and BC-Ch on skin wound healing were determined by rat models.

Histological examinations revealed that wounds treated with BC-Ch epithelialized and regenerated faster than groups treated with BC or Tegaderm (Lin, Lien, Yeh, Yu, & Hsu, 2013).

Carboxymethyl chitosan

Chitosan is a polysaccharide obtained from polymeric (1→4)-linked 2-amino-2-deoxy-β-D-glucopyranose units obtained by N-deacetylation of chitin. Because of its low allergenicity, biocompatibility, biodegradability, and non-toxicity, chitosan is widely used as a multipurpose biomaterial (Cheung, Ng, Wong, & Chan, 2015). Deacetylation of the amino groups in chitin produces chitosan, which is a plentiful polycationic biopolymer. The degree of deacetylation is usually greater than 50%. Due to protonation of amino groups, deacetylated amino groups allow chitosan to dissolve in dilute acids at pH less than 6.5 (Kalliola et al., 2018).

Because of the water-soluble limit, some active compounds in chitosan-containing formulations may degrade in the presence of acid solution and low pH. As a result, the preparation of chitosan derivative has been considered as a way to overcome the water-soluble limitation. Chitosan was carboxymethylated, resulting in carboxymethyl chitosan, which is soluble in a wide pH range. Because of their water solubility, carboxymethyl chitosan is used in a variety of fields including pharmaceuticals, cosmetics, food, agriculture, and medicine (Inamdar, Mourya, & Tiwari, 2010).

The degree of substitution of carboxymethylation depends on the concentration of base, amount of acid, type of solvent, nature of polymeric materials, reaction temperature, and reaction time. Because carboxymethyl chitosan has a higher polarity than chitosan, the degree of substitution increases, resulting in improved biopolymer water solubility. Carboxymethyl chitosan can be easily dissolved in water when made from chitosan powder with smaller particle sizes (Thanakkasaranee et al., 2021).

In fact, low molecular weight carboxymethyl chitosan is less than 50,000 Dalton (Da), medium molecular weight is 50,000 to 250,000 Da, and high molecular weight is more than 250,000 Da (de Farias et al., 2019).

Effect of molecular weight of carboxymethyl chitosan on the film properties. The film prepared from high molecular weight of carboxymethyl chitosan showed a higher thickness than from low molecular weight. The water vapor barrier properties of low molecular weight of carboxymethyl chitosan were higher than high molecular weight of carboxymethyl chitosan while medium molecular weight and low molecular weight showed a similar value. Low molecular weight carboxymethyl chitosan had higher water solubility than high molecular weight carboxymethyl chitosan. Moreover, water solubility is thus influenced by the degree of deacetylation (Bof, Bordagaray, Locaso, & García, 2015).

Mechanical property of carboxymethyl chitosan film strongly depended on its molecular weight. The film prepared from high molecular weight of carboxymethyl chitosan showed a higher tensile strength than the film prepared from low molecular weight of carboxymethyl chitosan (Bof et al., 2015).

CHAPTER III

RESEARCH METHODOLOGY

Chemicals and Medias

1. 0.25% Trypsin-EDTA (Lot. 2192415, Life Technologies Corporation, California, United States)
2. Acetonitrile (RCI Labscan Ltd, Bangkok, Thailand)
3. Agar (Seng huad limited, Bangkok, Thailand)
4. Aloe-emodin (Lot. W22IM-LQ, Tokyo Chemical Industry Co., Ltd, Tokyo, Japan)
5. Amphotericin B (Lot. 1607495, Life Technologies Corporation, New York, United States)
6. Calcium carbonate (Sigma-Aldrich, Missouri, United States)
7. Carboxymethyl chitosan (Lot. I1918, Mw: 100,000-300,000 Da, level of substitution: 95%, Santa Cruz Biotechnology, Inc., Texas, United States)
8. Citric acid (B/No. 1302135643, Ajax Finechem Pty Ltd, Auckland, New Zealand)
9. D-(+)-glucose anhydrous (Elago Enterprlses Pty Ltd, Cherrybrook, Australia)
10. Dimethyl sulfoxide (Lot#BCBV2983, Sigma-Aldrich, Missouri, United States)
11. Di-Sodium hydrogen phosphate (Elago Enterprlses Pty Ltd, Cherrybrook, Australia)
12. Dulbecco′s Modified Eagle Medium (Lot. 2180189, Life Technologies Corporation, New York, United States)
13. Electron-coupling reagent (Roche Diagnostics GmbH, Mannheim, Gemany)
14. Fetal bovine serum (Lot. 2232241, Life Technologies Corporation, California, United States)
15. Glycerin (Pacific Oleochemicals Sdn Bhd, Johor, Malaysia)
16. Lipopolysaccharides from Escherichia coli O26:B6 (Lot. #108M4192V, Sigma-Aldrich, Missouri, United States)

17. Methanol (RCI Labscan Ltd, Bangkok, Thailand)
18. Mouse TNF alpha uncoated ELISA kit (Lot. 218445-005, Thermo Fisher Scientific, Waltham, United States)
19. Orthophosphoric acid (B/No. 1707055160, Ajax Finechem Pty Ltd, Auckland, New Zealand)
20. Penicillin Streptomycin (Lot. 2321121, Life Technologies Corporation, New York, United States)
21. Peptone, Bacteriological (Lot. 0000437210, HiMedia Laboratories Pvt Ltd, Mumbai, India)
22. Phenoxyethanol (and) ethylhexylglycerin (Euxyl® PE 9010, Ashland Global Specialty Chemicals Inc, Delaware, United States)
23. Polyethylene glycol 400 (NOF Corporation, Tokyo, Japan)
24. Propylene glycol (Repsol Quimica SA, Madrid, Spain)
25. Sodium 3′-[1-(phenylaminocarbonyl)-3,4-tetrazolium]-bis (4-methoxy-6-nitro) benzene sulfonic acid hydrate (XTT) labeling reagent (Roche Diagnostics GmbH, Mannheim, Gemany)
26. Sodium bicarbonate (Lot. SLBT8842, Sigma-Aldrich, Missouri, United States)
27. Sodium hydroxide (B/No. 1702100417, Ajax Finechem Pty Ltd, Auckland, New Zealand)
28. Sorbitol solution 70% (Pure Chemical Corporation, Manila, Philippines)
29. Yeast extract powder (Lot.0000422827, HiMedia Laboratories Pvt Ltd, Mumbai, India)

Equipments

1. Autoclave (Tomy ES-315, Tomy Seiko Co., Ltd., Tokyo, Japan)
2. Benchtop centrifuge (Hettich Universal 320R, Andreas Hettich GmbH & co. KG, Tuttlingen, Germany)
3. Blender (Electrolux EBR3526, Electrolux (China) Home Appliance Co., Ltd, Beijing, China)
4. CO_2 incubator (Thermo Scientific Forma Steri-Cult, Thermo Fisher Scientific Inc., Massachusetts, United States)

5. Freeze drying apparatus (Christ Gamma 2-16 LSCplus, Martin Christ Gefriertrocknungsanlagen GmbH, Osterode am Harz, Germany)
6. High performance liquid chromatography system
   Detector (Shimadzu SPD-M10A, Shimadzu Corporation, Kyoto, Japan)
   Pump (Shimadzu LC-20AT, Shimadzu Corporation, Kyoto, Japan)
7. Hotplate stirrer (IKA RCT basic, IKA Werke GmbH & Co. KG, Staufen, Germany)
8. Incubator (Memmert IPP30, Memmert GmbH + Co. KG, Schwabach, Germany)
9. Inverted microscopes (Motic AE2000, Motic Hong Kong Limited, Kowloon Bay, Hong Kong)
10. Laminar air flow (Thermo Scientific 1300 Series A2, Thermo Fisher Scientific Inc., Massachusetts, United States)
11. Microplate reader (BioTek Eon, Biotek Instruments Inc., Vermont, United States)
12. pH meter (Mettler Toledo SevenCompact, Mettler toledo International Inc., Ohio, United States)
13. Plate shaker (CAPP CRP-412X, AHN Biotechnologie GmbH, Nordhausen, Germany)
14. Refrigerator (Snowland king of cool, Canon ball manufacturing Co., Ltd, Pathum thani, Thailand)
15. Scanning electron microscope (EDAX LEO1455VP, New Jersey, United States)
16. Shaking incubator (Drawell DW25-12DTS, Chongqing Drawell Instrument Co., Ltd., Chongqing, China)
17. Texture analyzer (TA.XT Plus, Stable Micro Systems Ltd, Godalming, United Kingdom)
18. Thickness gauge (Mitutoyo, Mitutoyo Corporation, kanagawa, Japan)
19. Ultracentrifuge (Beckman model J2-MC, Beckman Instruments Inc, Indiana, United States)
20. Ultrasonic cleaner (Branson 1510MT, Merck KGaA, Darmstadt, Germany)

21. Water bath (Memmert WNE 14, Memmert GmbH + Co. KG, Schwabach, Germany)
22. Water purification System (Milli-Q Direct, Merck KGaA, Darmstadt, Germany)

Methodologies

Preparation of aloe gel extract

The aloe gel extract preparation process was modified from the previous report (Inpanya, Faikrua, Ounaroon, Sittichokechaiwut, & Viyoch, 2012). Fresh leaves of *A. vera* were purchased from a garden in Phitsanulok and washed clean with tap water. The inner gel was collected, blended, and centrifuged at 12,000 rpm at 4°C for 15 min. The gel-like part was then lyophilized and kept at 4°C until required.

Reversed-phase high performance liquid chromatography (RP-HPLC) analysis of aloe-emodin in aloe gel extract

The aloe-emodin content in the extract was analyzed by RP-HPLC using a Shimadzu LC-20AT system. The separations were conducted at room temperature on a HyperClone (Phenomenex) (C18, 250 x 4.6 mm, 5µm) column using isocratic elution of acetonitrile (ACN): 0.1% aqueous phosphoric acid (1:1, v/v) in water at a flow rate of 1 mL/min. The signal of aloe-emodin was observed at 254 nm at a resolution of 4 nm using a photodiode array detector. The aloe-emodin content in the samples was quantified using a freshly prepared standard aloe-emodin as the calibration curve. The HPLC system was controlled, data were collected and integrated using LC solution software (Chiang et al., 2012).

Cell viability assay

This experiment followed the protocol approved by Naresuan University Institutional Biosafety Committee (NUIBC OT 64-08-29) using Raw 264.7 cells. Raw cells were seeded at a density of $1x10^4$ cells/well in 100 uL of DMEM with 10% FBS, antibiotics (100 U/mL of penicillin and 100 µg/mL streptomycin), and 250 µg/mL amphotericin B at 37°C in a 5% CO_2 incubator for 24 h. The medium was then replaced with serum-free DMEM with aloe gel extract at various concentrations (25,

50, 100 and 200 µg/mL). After 24 hours of treatment, XTT labeling and electron-coupling reagents were added to each well and incubated for 4 h. The absorbance was measured at 490 nm (Bancos, Tsai, Hackley, Weaver, & Tyner, 2012).

Anti-inflammatory activity of aloe gel extract

Raw 264.7 cells were seeded into 96-well plates ($1x10^4$ cells/well) for 24 h. They were treated with 1 µg/mL LPS and then treated by aloe gel extract at concentrations of 50, 100, and 200 µg/mL or aloe-emodin at concentrations of 0.85, 1.7, and 3.4 ng/mL, respectively, following which the tested cells were incubated at 37°C in a 5% CO_2 incubator for 24 h. The supernatants were then collected and TNF-α content was determined using the TNF-α ELISA kit (Zhao et al., 2013).

Preparation of bio-cellulose (BC)

BC was prepared from culture produced bacteria *G. xylinus* (TISTR 1064). The bacteria were divided into single colonies by cross streak on glucose yeast extract (GYE) agar containing 10% (w/v) glucose, 1% (w/v) yeast extract, 2% (w/v) agar and 1% (w/v) calcium carbonate and incubated at 30°C for 6-8 days. The single colonies of *G. xylinus* were moved into GYE broth containing 10% (w/v) glucose, 1% (w/v) yeast extract and shaken at 30°C for 48 h to produce the slurry bacterial cellulose (SBC). The SBC was placed into a sterile container containing Hestrin and Shcramm liquid medium consisting of 2% (w/v) glucose, 0.5% (w/v) bacto-peptone, 0.5% (w/v) yeast extract, 0.27% (w/v) di-sodium hydrogen phosphate and 0.115% (w/v) citric acid and pH adjusted to 4.5-4.6 with acetic acid. The medium was incubated at 30°C for 14 days in a static condition. At 14 days, the BC pellicle was collected and soaked in 0.25 M sodium hydroxide for 24 h to eliminate excess bacteria and the BC pellicle was washed with distilled water to neutralize pH. The BC was lyophilized and then kept in zip-lock plastic bags until used (Phimnuan et al., 2018).

Thickness of the BC

A thickness gauge was used to measure the thickness of BC membranes.

Mechanical properties of the BC

The mechanical properties of BC such as tensile strength and percent elongation at break were determined by using a texture analyzer. The BC membranes were cut into rectangular shape (10 mm x 50 mm). The distance between the grips was 30 mm and the crosshead rate was set at 1.00 mm/sec. Then, at least three samples in dried or wet (soak in water for 1 h) forms were tested. The tensile strength and elongation at break were calculated by following equation.

$$\text{Tensile strength (MPa)} = \frac{\text{Breaking force}}{\text{Cross section area of sample}}$$

and

$$\text{Elongation at break (\%)} = \frac{\text{Difference in length at breaking x 100}}{\text{Original length}}$$

Investigation of the surface and cross-section morphologies of the BC

The surface and cross-section morphologies of BC membranes were observed by scanning electron microscope (SEM).

Preparation of BC containing aloe gel extract

The uses and ingredients in each formulation are shown in Tables 4-5. The solution of carboxymethyl chitosan and aloe gel extract were prepared through the dissolution in distilled water. During the preparation of the mixture, plasticizers (propylene glycol, glycerin, polyethylene glycol 400 or 70% sorbitol) were added to increase the flexibility of formulation. In the last step, Phenoxyethanol (and) ethylhexylglycerin was added as a preservative. Afterwards, 5 mL of the mixture was added on lyophilized BC size 25 cm^2 for 1-2 h and left to dry at 37°C for 6-8 h. BC formulations were kept in a zip-lock plastic bag until used. All formulations were evaluated the thickness, mechanical properties and surface morphologies.

Table 4 Uses of ingredients in formulation of the BC containing aloe gel extract

Ingredients	Uses
Carboxymethyl chitosan	Film former
Aloe gel extract	Anti-inflammation
Glycerin	Plasticizer
Propylene glycol	Plasticizer
70% Sorbitol	Plasticizer
Polyethylene glycol 400	Plasticizer
Phenoxyethanol (and) ethylhexylglycerin	Preservative
Water	Solvent

Table 5 Formulation of the BC containing aloe gel extract solution

Ingredients	Amount (g)						
	F1	F2	F3	F4	F5	F6	F7
Carboxymethyl chitosan	0.5	0.2	0.1	0.2	0.2	0.2	0.2
Aloe gel extract	0.1	0.1	0.1	0.1	0.1	0.1	0.1
Glycerin	-	-	-	1	-	-	-
Propylene glycol	-	-	-	-	1	-	-
70% Sorbitol	-	-	-	-	-	1	-
Polyethylene glycol 400	-	-	-	-	-	-	1
Phenoxyethanol (and) ethylhexylglycerin	1	1	1	1	1	1	1
Water ad to	100	100	100	100	100	100	100

Stability testing

Samples of the formulation were kept in an aluminium foil bag or placed on a petri dish and stored either at 4°C or room temperature (24 ± 2°C) for 30 days for the stability test. The physical and mechanical properties of all samples were observed on day 0 and day 30 compared with freshly prepared formulation.

Release study

This method was adapted from the process previously reported (Phimnuan et al., 2018). The release study was performed by determination of the aloe-emodin in the BC. The BC was cut into 1 cm^2 shapes and soaked in 100 µL of the aloe gel extract at the concentration of 10 mg/mL for 1 h. Then, the saturated BC was submerged in 1 mL of water at 1, 5, 10, 15, 20 and 30 min. Then, the solutions were collected to determine aloe-emodin by the HPLC method as described above.

Statistical analysis

All data were expressed as mean ± standard deviation (SD). Student's t-test was used for comparison between two independent groups and one-way analysis of variance (ANOVA) followed by the Tukey's test was used for multiple comparisons using IBM SPSS statistic version 17.0 program. The *p*-value of less than 0.05 was considered as significance.

CHAPTER IV

RESULTS AND DISCUSSION

Preparation of aloe gel extract

The voucher herbarium specimen of aloe vera was stored at the faculty of Science Naresuan University (no. 005651). Many methods have been reported for the preparation of aloe vera extract at a high temperature (Kumar, Yadav, Yadav, Rohilla, & Yadav, 2017; Saniasiaya, Salim, Mohamad, & Harun, 2017) or at room temperature (Inpanya et al., 2012; Poosittisak & Wongkaew, 2016). The preparation method used in this research was adapted from the previous study (Inpanya et al., 2012) which heating was not used, heat may decrease the viscosity of the preparation and may decrease the biological effects of aloe gel extract. In this study, the aloe-emodin was found in the gel portion. In the extraction process, aloe-emodin, which has a low molecular weight, may bind to the polysaccharide, which has a high molecular weight. Therefore, the gel-like portion of the supernatant was collected.

The extract showed a cotton-like appearance (Figure 7) with a 0.6 % yield after lyophilization.

Figure 7 Appearance of aloe gel extract

HPLC analysis of aloe-emodin content

RP-HPLC is a suitable, general, and prevalent method for examining plants for the quantity and quality of their extracts (Kumar et al., 2017), and this was the

method that was used to quantify the amount of aloe-emodin in aloe gel extract. Aloe-emodin do not have readily ionizable groups, organic solvent/water mixtures were proved as optimum mobile phases. Both acetonitrile/water and methanol/water mixtures were justified to be appropriate for analyte compounds (Mandrioli et al., 2011). The water/acetonitrile system was shown to be the optimum mobile phase. When acid was added in the mobile phase, to reduce the peak tailing, a better separation was obtained (Xu et al., 2012).

The HPLC separation chromatogram showed an aloe-emodin peak at approximately 8.0 min (Figure 8A-C). The linear regression of the calibration curve of aloe-emodin was defined with y = 54648x - 59.446 and R^2 = 0.9937. The amount of aloe-emodin was calculated at 17.0 ± 3.1 µg/g of lyophilized extract. The aloe-emodin content is less than previously reported due to using dissimilar factors such as extract preparation, climate, and parts of use (Kumar et al., 2017).

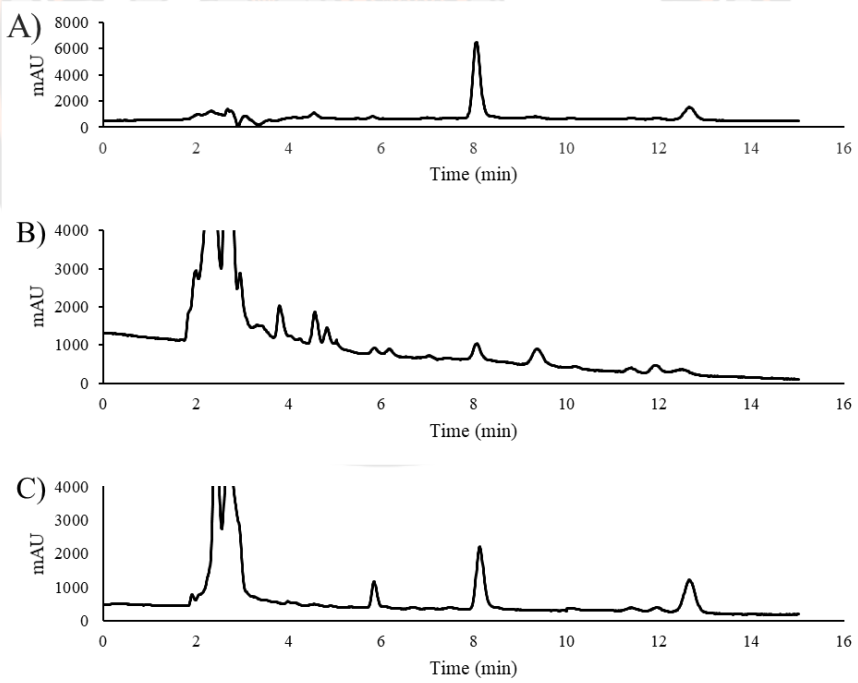

Figure 8 The HPLC chromatograms of (A) aloe-emodin standard 0.08 µg/mL (B) aloe-emodin in aloe gel extract at concentration 1000 µg/mL and (C) aloe-emodin in aloe gel extract at concentration of 1000 µg/mL spiked with aloe-emodin standard 33 µg/mL

Effect of aloe gel extract on the viability of Raw 264.7 macrophage cells

The XTT cell viability assay was used to determine the overall health of the Raw 264.7 macrophage cells. XTT was approved to be advantageous and easier to use than the 3-(4,5-Dimethylthiazol-2-yl)-2,5-Diphenyltetrazolium Bromide (MTT) method because the formazan product is water-soluble (Kuhn, Balkis, Chandra, Mukherjee, & Ghannoum, 2003). In the XTT test in this research, it was found that the increasing the concentration of aloe gel extract slightly decreased percentage viability of the cells, while aloe gel extract at 25-200 ug/mL was non-toxic to the cells (Figure 9). The highest concentration of aloe gel extract that yielded higher than 80% cell viability was 50-200 ug/mL which was used in the subsequent anti-inflammatory experiments.

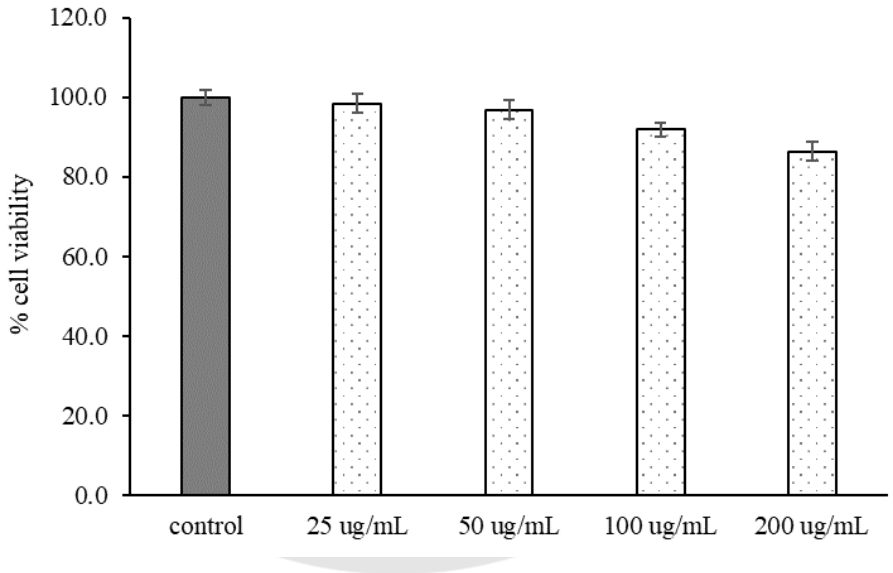

Figure 9 Cell viability of Raw 264.7 macrophage cells treated with aloe gel extract

Anti-inflammatory activity of the aloe gel extract

TNF-α is mainly a cytokine in the inflammatory process that is created by monocytes, macrophages, keratinocytes, and fibroblasts in the skin. UV radiation can also stimulate the generation of TNF-α by epidermal keratinocytes and dermal fibroblasts resulting in the enlargement of the area of inflammation. Furthermore, a

high amount of TNF-α enhances the synthesis of MMPs which leads to collagen production suppression (Borg et al., 2013).

To investigate the compounds of the aloe gel extract active in the generation of TNF-α, the aloe gel extract was cultured with a murine macrophage cell line using aloe-emodin as a marker in an equivalent amount in the extract.

The concentration of aloe gel extract that was found to assert the highest inhibition effect on the production of TNF-α was 200 ug/mL which significantly decreased the production of TNF-α in the LPS-activated murine macrophage cell line ($p < 0.05$) (Figure 10). The inhibition effect of the aloe gel extract was found to be higher than aloe-emodin at an equivalent amount of aloe-emodin (the aloe gel extract at 200 ug/mL equivalent to 3.4 ng/mL).

Because the aloe gel extract contained numerous active compounds such as acemannan (polysaccharide), lectins (protein), aloe-emodin (anthraquinone), and various vitamins, it was more effective at decreasing TNF-α than the pure compound. Furthermore, the pure compound contains only aloe-emodin. The combination of various compounds found in aloe gel extract may enhance the inhibitory effect on TNF-α production and resulted in a greater result than the use of a single compound.

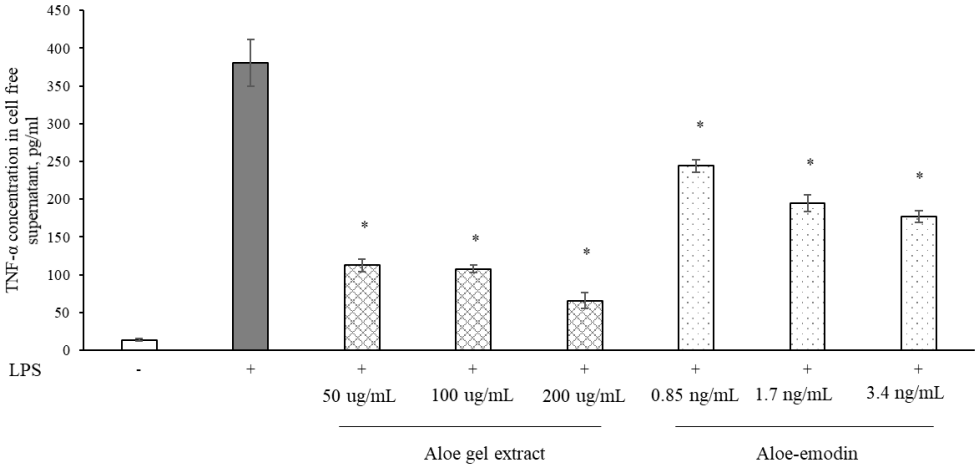

Figure 10 The effect of aloe gel extract and aloe-emodin on the production of TNF-α in Raw 264.7 macrophage cells. The data was represented as mean ± SD. One-way ANOVA indicates significantly different (*$p < 0.05$) from the cells treated with only LPS.

Aloe gel extract has been shown to have the potential to reduce TNF-α content during the preparation and evaluation of anti-inflammatory activity. As a result, the next step was to prepare BC and combine it with aloe gel extract. Because the aloe extract's primary component is polysaccharide, it is unstable and easily degraded. As a result, dry formulations can help maintain the active compound's stability.

Preparation and characteristics of BC

G. xylinus was cultured in GYE broth for 14 days at which point BC was produced on the top surface of the production medium. The characteristics of the BC was white, round-shaped (depending on the container), jelly-like, and elastic with a thickness of approximately 1 mm. After lyophilization, the BC was dry, white with a thickness of approximately 0.1 mm, as shown in Figure 11A-B. The tensile strength of the dried BC was 11.67 ± 0.66 and the wet BC, 4.39 ± 0.87 MPa. The percentage elongation at break of the dried BC was 6.54 ± 0.77 and of the wet BC, 12.88 ± 0.63 %. The tensile strength of the dried BC was reported as 5.91 ± 0.79 and 2.61 ± 0.93 MPa for the wet BC, in a previous study (Phimnuan et al., 2018), which were lower than the BC in our study. Nevertheless, the values may vary due to different conditions such as culture time, source of bacteria, and thickness of the BC before lyophilization (Lin et al., 2013).

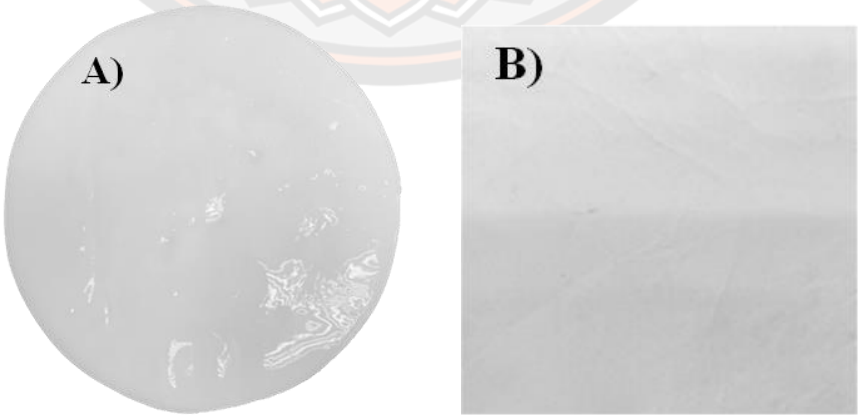

Figure 11 Appearance of the BC (A) after prepared from culture produced bacteria and (B) after lyophilized

As illustrated in Figure 12, the tensile strength of the BC in dried form was significantly higher than wet form at $p < 0.05$. This was due to water penetrating the gaps of the cellulose fibers which causes the bonds between the cellulose fibers to break. As a result, the strength of the wet BC is reduced. Figure 13 shows the graph of elongation at break which the BC in dried form was significantly less than the BC in wet form at $p < 0.05$ due to the attachment between the water molecules and cellulose fibers which lead to swelling of the fibers. As a result, the flexibility of the wet BC increased.

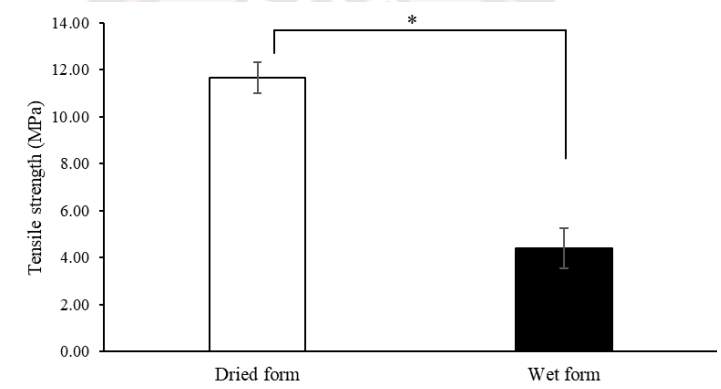

Figure 12 Tensile strength of the BC at dried and wet form. Each bar represents mean ± SD. Student's t-test indicates significantly different (*$p < 0.05$) between two groups.

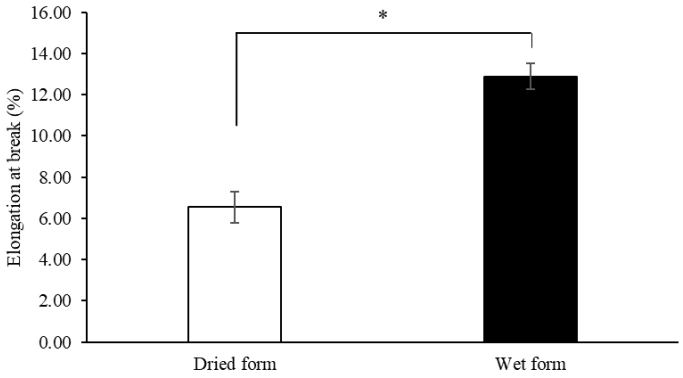

Figure 13 Elongation at break of the BC at dried and wet form. Each bar represents mean ± SD. Student's t-test indicates significantly different (*$p < 0.05$) between two groups.

The surface and cross-section morphology of the BC membranes were observed by SEM. Lyophilized BC has a three-dimensional structure of nanofibrils which is highly uniaxially oriented and porous (Figure 14A) found on the surface of the BC membrane (Maneerung, Tokura, & Rujiravanit, 2008). However, the multiple layers of the BC membranes are connected by the nanofibrils, as shown in the cross-sectional morphology of BC illustrated in Figure 14B. This occurs in the process of BC pellicle growth where bacteria create cellulose only in the proximity of the culture surface. The BC pellicle is suspended by the adherence to the wall of the container and slips steadily downwards as it thickens (Maneerung et al., 2008). Based on the literature, β-(1→4) glucan chains were polymerized by bacteria that were organized and stabilized by intra-/inter-molecular hydrogen bonds to produce an ultrafine reticulated structure (Esa et al., 2014). Our findings regarding the BC membranes were in agreement with the literature. This unique morphology leads to the ability to hold a large amount of water while also exhibiting great elasticity (Maneerung et al., 2008).

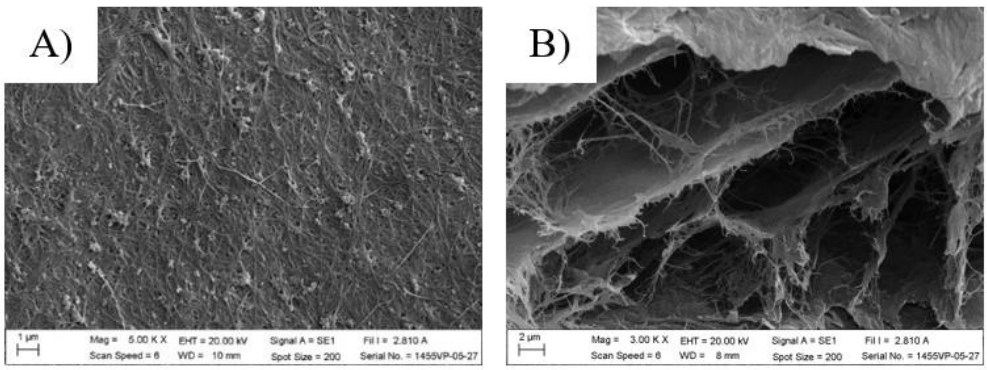

Figure 14 SEM image of (A) surface morphology and (B) cross section morphology

In the formulation of this study, carboxymethyl chitosan was used as a film former, aloe gel extract was used as an anti-inflammatory active ingredient, glycerin, propylene glycol, 70% sorbitol, and polyethylene glycol 400 were used as plasticizers, and a mixture of phenoxyethanol and ethylhexylglycerin was used as a preservative.

Preparation and characteristics of BC containing aloe gel extract

Formulation 1 to 3

Because chitosan is a biodegradable natural polymer with many unique properties such as the ability to form films, chelate metal ions, and optical structural characteristics, it was chosen in the formulation. Furthermore, chitosan has several beneficial properties, including biorenewability, biodegradability, biocompatibility, bioadhesivity, and non-toxicity, making it suitable for use in cosmetics (Jimtaisong & Saewan, 2013).

Chitosan, on the other hand, has low water solubility. It must be soluble in acidic water. The active compound may be degraded due to acid sensitivity when it was used in formulations. As a result, chitosan derivative such as carboxymethyl chitosan, is intriguing. Furthermore, carboxymethyl chitosan has a positive charge while BC has a negative charge. It could be complex and aid in the attachment of the active compound of aloe gel extract to BC. To obtain a clear solution, the percentage of carboxymethyl chitosan was used in the range of 0.1-0.5%.

In this study, the carboxymethyl chitosan with a molecular weight of 100,000-300,000 Da, a 95% substitution level, and a 90% degree of deacetylation was used. O-carboxymethylation is the main product. Low molecular weight carboxymethyl chitosan is less than 50,000 Da, medium molecular weight is 50,000 to 250,000 Da, and the high molecular weight is more than 250,000 Da (de Farias et al., 2019). A previous study discovered that film made with high molecular weight carboxymethyl chitosan had higher tensile strength than film made with low molecular weight carboxymethyl chitosan (Thanakkasaranee et al., 2021).

The degree of substitution affected the water solubility of carboxymethyl chitosan. Water solubility and water vapor transmission rates were higher in the film made with carboxymethyl chitosan with a high degree of substitution (Thanakkasaranee et al., 2021).

The BC containing aloe gel extract, which was easy to prepare, was white and opaque with a thickness of approximately 0.1 mm. The concentrations of carboxymethyl chitosan in Formulations 1-3 were varied. The thickness of formulation 1-3 is shown in Table 6. The physical appearance of each formulation is shown in Figure 15A-C. Tensile strength and percentage elongation at break of each

formulation are shown in Figures 16-17. It was shown that the addition of a higher amount of carboxymethyl chitosan increased the hardness, thickness and tensile strength of BC. As shown in Figure 16, Formulation 2 and Formulation 3 significantly higher tensile strength than Formulation 1 at $p < 0.05$. However, Formulation 3 with 0.5% carboxymethyl chitosan had the highest tensile strength. Carboxymethyl chitosan may penetrate inside the empty pores of BC and interact with the microfibrils, which may affect the density of the structure. For elongation at break, each formulation was no different. Carboxymethyl chitosan did not affect the flexibility of the formulation. However, Formulation 2 with 0.2% carboxymethyl chitosan gave the optimum hardness and was chosen as the formulation for further study.

Table 6 The thickness of BC patch, formulation 1-3

Formulations	**F1**	**F2**	**F3**
Thickness (mm)	0.11 ± 0.04	0.13 ± 0.05	0.17 ± 0.07

Figure 15 physical appearance of BC patch, formulation 1-3 varied the amount of carboxymethyl chitosan at concentration (A) 0.1% (B) 0.2% and (C) 0.5%

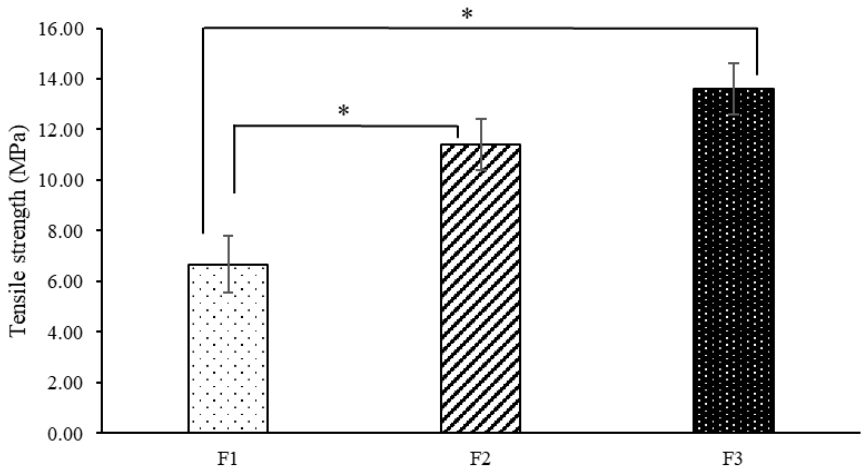

Figure 16 Tensile strength of BC patch, formulation 1-3. Each bar represents mean ± SD. One-way ANOVA indicates significantly different (*$p < 0.05$) between two groups.

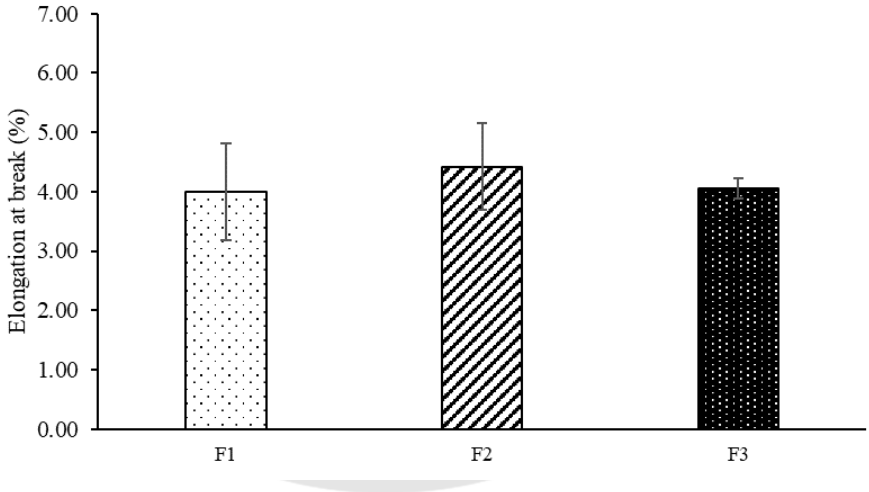

Figure 17 Elongation at break of BC patch, formulation 1-3. Each bar represents mean ± SD.

Note: F1 = 0.1% carboxymethyl chitosan

F2 = 0.2% carboxymethyl chitosan

F3 = 0.5% carboxymethyl chitosan

Formulation 4 to 7

Each of the formulations 4-7 contained 0.2% carboxymethyl chitosan, aloe gel extract, phenoxyethanol and ethylhexylglycerin, but each contained a different plasticizer: glycerin, propylene glycol, 70% sorbitol, and polyethylene glycol 400 were used in Formulation 4-7, respectively. The physical appearance of each formulation is shown in Figure 18A-D. Formulation 5 had a homogeneous appearance which was different to the other formulations.

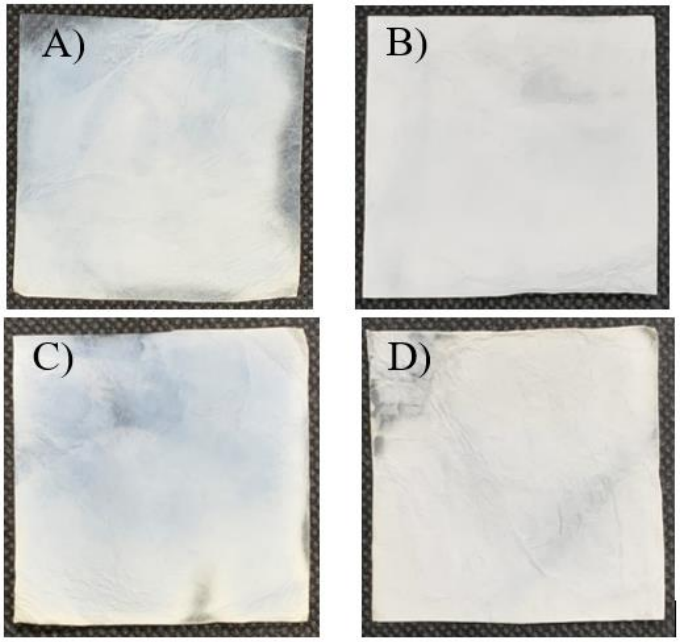

Figure 18 physical appearance of BC patch, formulation 4-7 varied type of plasticizers by (A) glycerin (B) propylene glycol (C) 70% sorbitol and (D) polyethylene glycol 400

The thickness of formulation 4-7 is shown in Table 7. Tensile strength and elongation at break were determined for each formulation. Plasticizers with lower molecular weights can easily interact with the molecular chains of polymers. This is demonstrated in Figure 19, where the significant difference indicates that Formulations 4, 5 and 7 had a higher tensile strength than Formulation 6 at $p < 0.05$. However, Formulation 5 which was homogeneous appearance had the highest tensile strength.

Table 7 The thickness of BC patch, formulation 4-7

Formulation	F4	F5	F6	F7
Thickness (mm)	0.13 ± 0.05	0.11 ± 0.03	0.10 ± 0.05	0.12 ± 0.03

Figure 19 also illustrates that propylene glycol (76.09 g/mol) has higher efficacy in plasticizing BC than all of the glycerin (92.09 g/mol), sorbitol (182.17 g/mol), and polyethylene glycol 400 (380-420 g/mol). Other researchers have also reported a similar result with other polysaccharides where propylene glycol gave greater tensile strength than other polyols (Jantrawut, Chaiwarit, Jantanasakulwong, Brachais, & Chambin, 2017).

The percentage elongation value indicates the elasticity of the formulations. Figure 20 shows the percentage elongation at break of the formulations 4-7. The formulation with glycerin gave the highest percentage elongation at break. The elongation of polymers relies on the mobility between the molecular chains. The plasticizers can increase elasticity in BC due to the plasticizers reducing the intermolecular bonds and substituting them with hydrogen bonds formed between the plasticizer and the BC molecules. The Reconstruction of BC molecular bonding decreases rigidity and increases the elasticity of BC caused by easy mobility (Sanyang, Sapuan, Jawaid, Ishak, & Sahari, 2015).

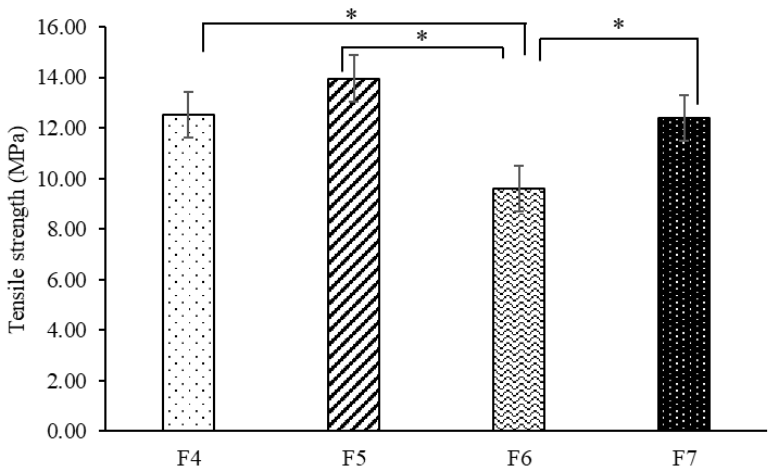

Figure 19 Tensile strength of BC patch, formulation 4-7. Each bar represents mean ± SD. One-way ANOVA indicates significantly different (*$p < 0.05$) between two groups.

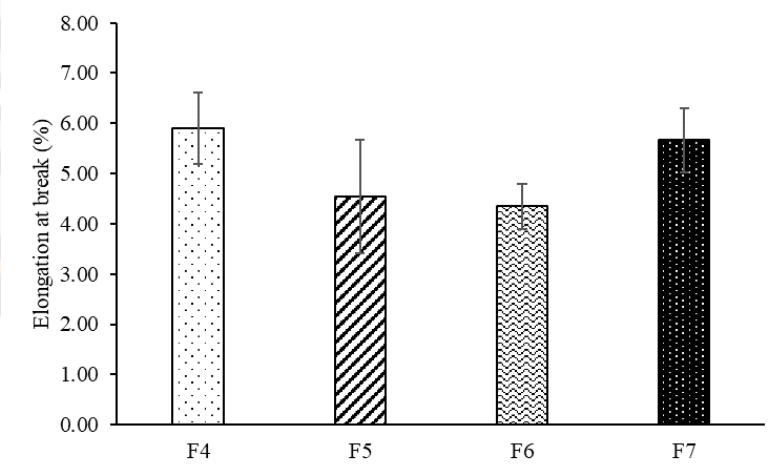

Figure 20 Elongation at break of BC patch, formulation 4-7. Each bar represents mean ± SD.

Note: F4 = glycerin

F5 = propylene glycol

F6 = 70% Sorbitol

F7 = Polyethylene glycol 400

Figure 21 shows an SEM image of formulation 4-7. BC has a highly porous nanofibril structure. These results make BC incorporate the substances such as aloe gel extract that are attached to the cellulose fibers. The addition of plasticizer made the network less compacted because the presence of plasticizer limited the extent of the collapse of the three-dimensional structure of BC during drying.

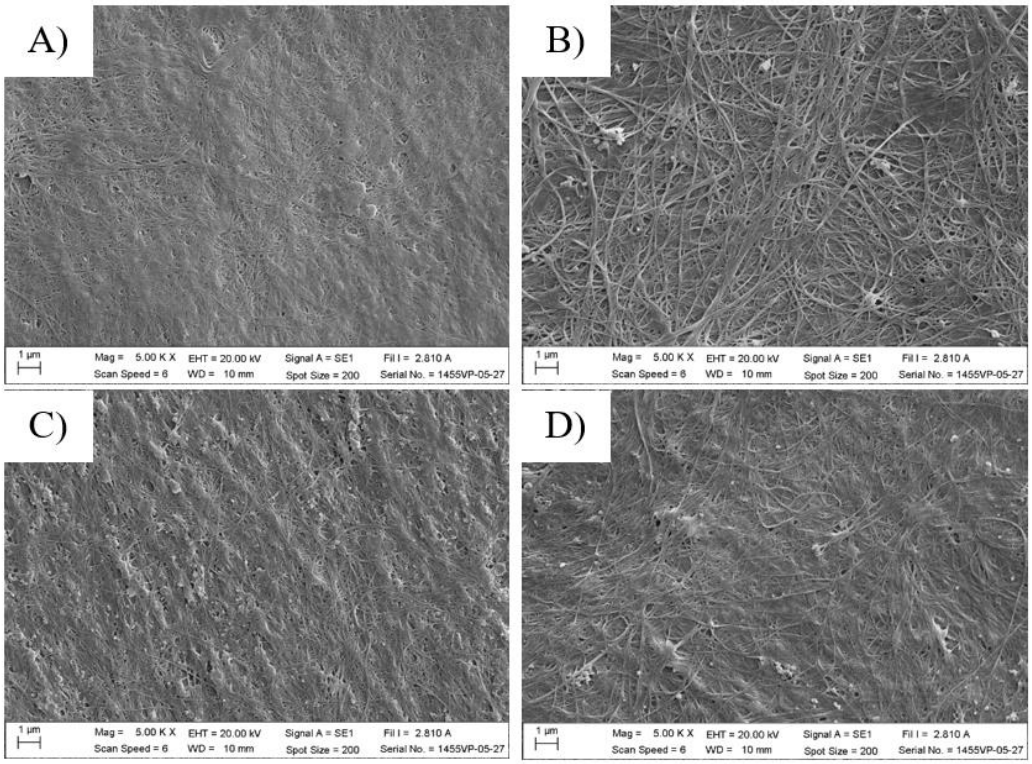

Figure 21 SEM image of BC patch, formulation 4-7 by (A) glycerin (B) propylene glycol (C) 70% sorbitol and (D) polyethylene glycol 400

These results revealed that glycerin and propylene glycol would be a good option due to plasticizers interacting with water to promote limpness and elasticity. Propylene glycol is the highest efficacy plasticizer in improving the tensile strength and the physical appearance of the BC, and increasing flexibility. So, Formulation 5 consisting of aloe gel extract as well as 0.2% carboxymethyl chitosan and propylene glycol was chosen for stability testing. The ingredient in Formulation 5 is shown in Table 8.

Table 8 The ingredients in Formulation 5

Ingredients	Amount (g)
Carboxymethyl chitosan	0.2
Aloe gel extract	0.1
Propylene glycol	1
Phenoxyethanol (and) ethylhexylglycerin	1
Water ad to	100

Stability testing

Stability testing of the BC containing aloe gel extract was conducted for one month at different temperature conditions such as 4°C and room temperature (24 ± 2°C). The results were summarized in Table 9. The physical appearance and mechanical properties were evaluated compared to freshly prepared formulations. BC membranes were kept in an aluminium foil bag or placed on a petri dish. The physical properties of the BC in the aluminium foil bags, such as color, visual texture, and texture feeling, did not change. Tensile strength and percentage elongation at the break also did not change. In contrast, the BC on the petri dish retained the white color (Figure 22) but the texture and mechanical properties of BC were changed. The tensile strength of the BC on the petri dish at room temperature significantly decreased with $p < 0.05$ when compared with the freshly prepared formulations. The chemical properties of Formulation 5 could not be analyzed because approximately 0.7675 g of the solution was absorbed into the BC and the residual amount of aloe-emodin in aloe gel extract was too small to be detected by HPLC. Given this, we recommend increasing the dose of aloe gel extract in the formulation. Nonetheless, the results from the stability testing suggested that Formulation 5 provided good stability of both its physical and mechanical properties during storage. The recommended packaging should be moisture-proof and well-sealed.

Table 9 Summary of physical and mechanical properties of the BC containing aloe gel extract

Evaluations	Freshly prepared	Packaging			
		With packaging		Without packaging	
		RT	4°C	RT	4°C
Color	White	White	White	White	White
Thickness (mm)	0.11 ± 0.03	0.12 ± 0.05	0.13 ± 0.02	0.12 ± 0.02	0.13 ± 0.02
Tensile strength (MPa)	13.96 ± 1.02	12.66 ± 1.70	12.23 ± 1.98	8.55 ± 1.49*	11.47 ± 0.84
Elongation at break (%)	4.54 ± 1.12	4.66 ± 0.32	4.92 ± 0.89	3.96 ± 0.09	4.15 ± 0.33

Note: one-way ANOVA indicates significantly different (*$p < 0.05$) when compared with the freshly prepared formulations.

RT = room temperature

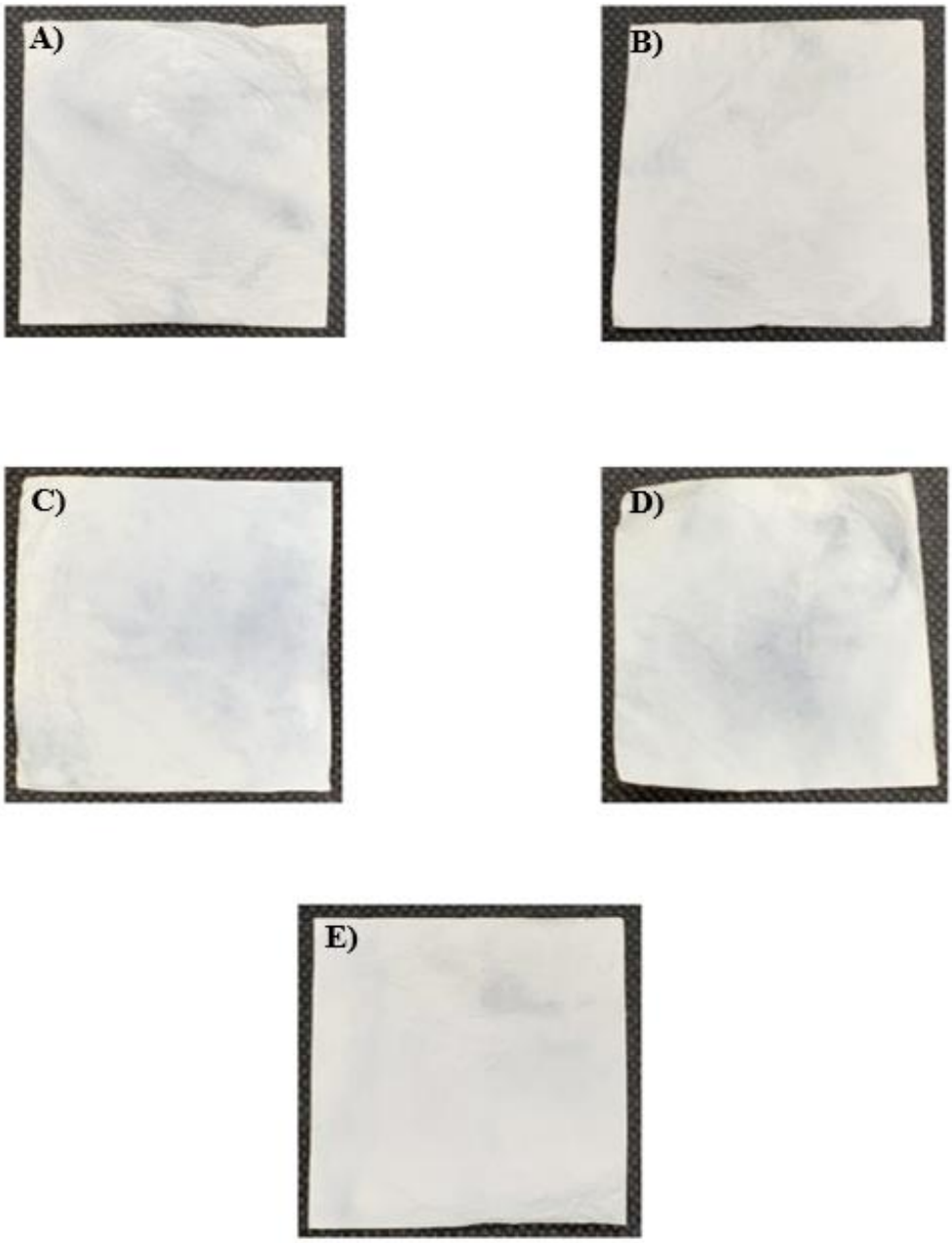

Figure 22 physical appearance of BC patch, Formulation 5 after (A) kept at RT with packaging (B) kept at 4°C with packaging (C) kept at RT by placed on a petri dish (D) kept at 4°C by placed on a petri dish for 1 month and (E) freshly prepared formulation

Release study

The HPLC method was used to calculate the amount of aloe-emodin released from the BC, which is shown in Figure 23 as ng/cm^2. The linear regression of the calibration curve of aloe-emodin was defined with y = 55238x - 167.14 and R^2 = 0.9741. Initially, 1 mg of aloe gel extract was used (the aloe gel extract 1 mg equivalent to aloe-emodin 17 ng). At 1 minute, 2.37 ± 0.20 ng of aloe-emodin were detected. After 10 minutes, the aloe-emodin concentration remained relatively stable. Aloe-emodin was released in a time-dependent manner. At 30 minutes, the calculated amount of aloe-emodin was 5.86 ± 0.56 ng. As a result, the recommended concentration of aloe gel extract in Formulation 5 is 3.26%. The results of the release study indicated that the amount of aloe gel extract to use in Formulation 5 should be investigated further.

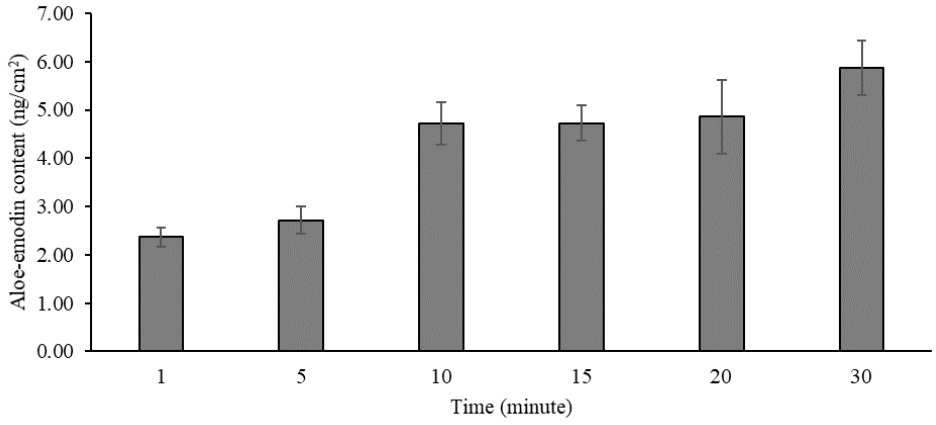

Figure 23 Release study of aloe-emodin in BC 1x1 cm^2 with the amount of aloe gel extract 1 mg at various times. Each bar represents mean ± SD.

CHAPTER V

CONCLUSION

In this study, the aloe gel extract demonstrated a cotton-like texture with 0.6 % yield after lyophilization. HPLC analysis calculated the amount of aloe-emodin as 17.0 ± 3.1 μg/g of dried extract. In the XTT assay in this research, it was found that increasing the doses of aloe gel extract slightly decreased percentage viability of the cells, while aloe gel extract at a concentration of 25-200 ug/mL was non-toxic. At concentration 200 ug/mL, the extract yielded higher than 80% cell viability. So, 50-200 ug/mL was used in the anti-inflammatory experiments. The highest inhibition effect on the production of TNF-α, was with 200 ug/mL aloe gel extract. The aloe gel extract significantly reduced the production of TNF-α in LPS-activated Raw 264.7 cells with $p < 0.05$. The inhibition effect of the aloe gel extract was found to be higher than aloe-emodin at an equivalent amount of aloe-emodin (the aloe gel extract at 200 ug/mL equivalent to 3.4 ng/mL).

The characteristics of the BC that was prepared from bacteria *G. xylinus* were a white round shape (depending on container), jelly-like, elastic, and with a thickness of approximately 1 mm. After lyophilization, the BC was dry, white, and approximately 0.1 mm thick. The morphology from the SEM showed three-dimensional structures of nanofibrils which were highly uniaxially oriented. Our findings regarding the BC membranes are in agreement with the literature.

The formulation of BC using 0.2% carboxymethyl chitosan gave the optimum hardness and was chosen for further study. The formulation of BC containing aloe gel extract showed that propylene glycol is the most efficacious plasticizer for improving the tensile strength and the physical appearance of the formulations, with increasing flexibility. So, Formulation 5 consisting of aloe gel extract as well as 0.2% carboxymethyl chitosan and propylene glycol was chosen for stability testing. The results from the stability testing of this formulation indicate that it provided good stability of both the physical and mechanical properties during storage. As well, the release of the aloe gel extract from the BC was found to be time-

dependent. The recommended amount of aloe gel extract in Formulation 5 should be 3.26%.

It can therefore be concluded from the results of this study that BC containing of aloe gel extract has good potential for use in anti-photoaging cosmetic products such as eye patches or face masks.

Suggestions

1. Stability testing should be undertaken on the chemical and microbial properties of the formulations.
2. Skin permeation testing to determine the permeation of a compound through the skin should also be performed to obtain information about the behavior of a test substance when applied to the skin's surface.

REFERENCES

Bancos, S., Tsai, D. H., Hackley, V., Weaver, J. L., & Tyner, K. M. (2012). Evaluation of viability and proliferation profiles on macrophages treated with silica nanoparticles *in vitro* via plate-based, flow cytometry, and coulter counter assays. *ISRN Nanotechnology, 2012,* 454072.

Bof, J., Bordagaray, V., Locaso, D., & García, M. (2015). Chitosan molecular weight effect on starch-composite film properties. *Food Hydrocolloids, 51*, 281-294.

Borg, M., Brincat, S., Camilleri, G., Schembri-Wismayer, P., Brincat, M., & Calleja-Agius, J. (2013). The role of cytokines in skin aging. *Climacteric, 16*(5), 514-521.

Brandão, M., Araújo, L., Araújo, A., Santos, M., & Miguel, M. (2016). Evaluation of wound healing treated with latex derived from rubber trees and *Aloe vera* extract in rats. *Acta Cirurgica Brasileira, 31,* 570-577.

Bruunsgaard, H., Skinhøj, P., Pedersen, A. N., Schroll, M., & Pedersen, B. K. (2000). Ageing, tumour necrosis factor-alpha (TNF-alpha) and atherosclerosis. *Clinical and experimental immunology, 121*(2), 255-260.

Cataldi, V., Di Bartolomeo, S., Di Campli, E., Nostro, A., Cellini, L., & Di Giulio, M. (2015). *In vitro* activity of *Aloe vera* inner gel against microorganisms grown in planktonic and sessile phases. *Int J Immunopathol Pharmacol, 28*(4), 595-602.

Cherukuri, S., Kiranmai, M., Cherukuri, V., & Ganapuram, K. (2017). Formulation and evaluation of transdermal drug delivery of topiramate. *International Journal of Pharmaceutical Investigation, 7*, 10-17.

Cheung, R. C., Ng, T. B., Wong, J. H., & Chan, W. Y. (2015). Chitosan: an update on potential biomedical and pharmaceutical applications. *Marine drugs, 13*(8), 5156-5186.

Chiang, H. M., Lin, Y. T., Hsiao, P. L., Su, Y. H., Tsao, H. T., & Wen, K. C. (2012). Determination of marked components -aloin and aloe-emodin- in aloe vera before and after hydrolysis. *Journal of Food and Drug Analysis, 20*, 646-652.

Chithra, P., Sajithlal, G. B., & Chandrakasan, G. (1998). Influence of aloe vera on collagen characteristics in healing dermal wounds in rats. *Mol Cell Biochem, 181*(1-2), 71-76.

Choi, J. W., Lee, J., & Park, Y. I. (2017). 7,8-Dihydroxyflavone attenuates TNF-α-induced skin aging in Hs68 human dermal fibroblast cells via down-regulation of the MAPKs/Akt signaling pathways. *Biomedicine & Pharmacotherapy, 95*, 1580-1587.

de Farias, B. S., Grundmann, D. D. R., Rizzi, F. Z., Martins, N. S. S., Sant'Anna Cadaval Junior, T. R., & de Almeida Pinto, L. A. (2019). Production of low molecular weight chitosan by acid and oxidative pathways: effect on physicochemical properties. *Food Research International, 123*, 88-94.

Draelos, Z. D. (2006). Concepts in a multiprong approach to photoaging. *Skin therapy letter, 11*(3), 1-3.

Esa, F., Tasirin, S. M., & Rahman, N. A. (2014). Overview of bacterial cellulose production and application. *Agriculture and Agricultural Science Procedia, 2*, 113-119.

Farage, M. A., Miller, K. W., Elsner, P., & Maibach, H. I. (2008). Intrinsic and extrinsic factors in skin ageing: a review. *Int J Cosmet Sci, 30*(2), 87-95.

Fisher, G. J. (2005). The pathophysiology of photoaging of the skin. *Cutis, 75*(2 Suppl), 5-8; discussion 8-9.

Fisher, G. J., Kang, S., Varani, J., Bata-Csorgo, Z., Wan, Y., Datta, S., & Voorhees, J. J. (2002). Mechanisms of photoaging and chronological skin aging. *Archives of Dermatology, 138*(11), 1462-1470.

Fuller, B. (2019). Role of PGE-2 and other inflammatory mediators in skin aging and their inhibition by topical natural anti-inflammatories. *Cosmetics, 6*(1), 6.

Goudarzi, M., Fazeli, M., Azad, M., Seyedjavadi, S. S., & Mousavi, R. (2015). *Aloe vera* gel: effective therapeutic agent against multidrug-resistant *Pseudomonas aeruginosa* isolates recovered from burn wound infections. *Chemotherapy Research and Practice, 2015*, 639806.

Goukassian, D. A., & Gilchrest, B. A. (2004). The interdependence of skin aging, skin cancer, and DNA repair capacity: a novel perspective with therapeutic implications. *Rejuvenation Res, 7*(3), 175-185.

Halib, N., Mohd Amin, M. C. I., & Ahmad, I. (2012). Physicochemical properties and characterization of nata de coco from local food industries as a source of

cellulose. *Sains Malaysiana, 41*, 205-211.

Hamman, J. H. (2008). Composition and applications of aloe vera leaf gel. *Molecules, 13*(8), 1599-1616.

Harhaji, L., Mijatovic, S., Maksimovic-Ivanic, D., Popadic, D., Isakovic, A., Todorovic-Markovic, B., & Trajkovic, V. (2007). Aloe emodin inhibits the cytotoxic action of tumor necrosis factor. *European Journal of Pharmacology, 568*(1), 248-259.

Inamdar, N., Mourya, V. K., & Tiwari, A. (2010). Carboxymethyl chitosan and its applications. *Advanced Material Letters, 1*, 11-33.

Inpanya, P., Faikrua, A., Ounaroon, A., Sittichokechaiwut, A., & Viyoch, J. (2012). Effects of the blended fibroin/aloe gel film on wound healing in streptozotocin-induced diabetic rats. *Biomedical Materials, 7*, 035008.

Jantrawut, P., Chaiwarit, T., Jantanasakulwong, K., Brachais, C., & Chambin, O. (2017). Effect of plasticizer type on tensile property and *in vitro* indomethacin release of thin films based on low-methoxyl pectin. *Polymers, 9*, 289.

Jimtaisong, A., & Saewan, N. (2013). Utilization of carboxymethyl chitosan in cosmetics. *Int J Cosmet Sci, 36*, 12-21.

Kalliola, S., Repo, E., Srivastava, V., Zhao, F., Heiskanen, J. P., Sirviö, J. A., . . . Sillanpää, M. (2018). Carboxymethyl chitosan and its hydrophobically modified derivative as pH-switchable emulsifiers. *Langmuir : the ACS journal of surfaces and colloids, 34*(8), 2800-2806.

Kammeyer, A., & Luiten, R. M. (2015). Oxidation events and skin aging. *Ageing Research Reviews, 21*, 16-29.

Kawasumi, A., Sagawa, N., Hayashi, S., Yokoyama, H., & Tamura, K. (2012). Wound healing in mammals and amphibians: toward limb regeneration in mammals. *Current topics in microbiology and immunology, 367*, 33-49.

Kennedy, C., Bastiaens, M. T., Bajdik, C. D., Willemze, R., Westendorp, R. G., & Bouwes Bavinck, J. N. (2003). Effect of smoking and sun on the aging skin. *Journal of Investigative Dermatology, 120*(4), 548-554.

Kuhn, D. M., Balkis, M., Chandra, J., Mukherjee, P. K., & Ghannoum, M. A. (2003). Uses and limitations of the XTT assay in studies of Candida growth and metabolism. *Journal of clinical microbiology, 41*(1), 506-508.

Kumar, S., Yadav, M., Yadav, A., Rohilla, P., & Yadav, J. P. (2017). Antiplasmodial potential and quantification of aloin and aloe-emodin in *Aloe vera* collected from different climatic regions of India. *BMC complementary and alternative medicine, 17*(1), 369-369.

Leow, Y. H., & Maibach, H. I. (1998). Cigarette smoking, cutaneous vasculature, and tissue oxygen. *Clin Dermatol, 16*(5), 579-584.

Lin, W. C., Lien, C. C., Yeh, H. J., Yu, C. M., & Hsu, S. H. (2013). Bacterial cellulose and bacterial cellulose–chitosan membranes for wound dressing applications. *Carbohydrate Polymers, 94*(1), 603-611.

Maan, A., Nazir, A., Khan, M., Ahmad, T., Zia, R., Murid, M., & Abrar, M. (2018). The therapeutic properties and applications of *Aloe vera* : A review. *Journal of Herbal Medicine, 12*, 1-10.

Mandrioli, R., Mercolini, L., Ferranti, A., Fanali, S., & Raggi, M. A. (2011). Determination of aloe emodin in Aloe vera extracts and commercial formulations by HPLC with tandem UV absorption and fluorescence detection. *Food Chemistry, 126*(1), 387-393.

Maneerung, T., Tokura, S., & Rujiravanit, R. (2008). Impregnation of silver nanoparticles into bacterial cellulose for antimicrobial wound dressing. *Carbohydrate Polymers, 72*, 43-51.

Narayanan, S., Jadhav, A. P., & Kadam, V. J. (2015). Forced degradation studies of aloe emodin and emodin by HPTLC. *Indian J Pharm Sci, 77*(6), 795-798.

Pacheco, G., de Mello, C. V., Chiari-Andréo, B. G., Isaac, V. L. B., Ribeiro, S. J. L., Pecoraro, É., & Trovatti, E. (2018). Bacterial cellulose skin masks-properties and sensory tests. *J Cosmet Dermatol, 17*(5), 840-847.

Park, M. Y., Kwon, H. J., & Sung, M. K. (2009). Evaluation of aloin and aloe-emodin as anti-inflammatory agents in aloe by using murine macrophages. *Bioscience, Biotechnology, and Biochemistry, 73*(4), 828-832.

Perugini, P., Bleve, M., Cortinovis, F., & Colpani, A. (2018). Biocellulose masks as delivery systems: a novel methodological approach to assure quality and safety. *Cosmetics, 5*, 66.

Phimnuan, P., Yakaew, S., Faikrua, A., Luangbudnak, W., Grandmottet, F., & Viyoch,

J. (2018). Development of anti-acne film from bio-cellulose incorporating *Punica granatum* peel extract. *Walailak Journal of Science and Technology (WJST), 16*, 765-778.

Pillai, S., Oresajo, C., & Hayward, J. (2005). Ultraviolet radiation and skin aging: roles of reactive oxygen species, inflammation and protease activation, and strategies for prevention of inflammation-induced matrix degradation - a review. *Int J Cosmet Sci, 27*(1), 17-34.

Poon, F., Kang, S., & Chien, A. L. (2015). Mechanisms and treatments of photoaging. *Photodermatology, Photoimmunology and Photomedicine, 31*(2), 65-74.

Poosittisak, S., & Wongkaew, P. (2016). Electrochemical study of aloe gel and emodin on a screen printed carbon electrode. *International Journal of GEOMATE, 11*, 2815-2819.

Rezazadeh, F., Moshaverinia, M., Motamedifar, M., & Alyaseri, M. (2016). Assessment of anti HSV-1 activity of aloe vera gel extract: an in vitro study. *Journal of Dentistry (Shiraz), 17*(1), 49-54.

Rinnerthaler, M., Bischof, J., Streubel, M. K., Trost, A., & Richter, K. (2015). Oxidative stress in aging human skin. *Biomolecules, 5*(2), 545-589.

Ritsu, M., Kawakami, K., Kanno, E., Tanno, H., Ishii, K., Imai, Y., . . . Tachi, M. (2017). Critical role of tumor necrosis factor-α in the early process of wound healing in skin. *Journal of Dermatology & Dermatologic Surgery, 21*(1), 14-19.

Rittié, L., & Fisher, G. J. (2015). Natural and sun-induced aging of human skin. *Cold Spring Harb Perspect Med, 5*(1), a015370.

Ruka, D. R., Simon, G. P., & Dean, K. M. (2012). Altering the growth conditions of *Gluconacetobacter xylinus* to maximize the yield of bacterial cellulose. *Carbohydrate Polymers, 89*(2), 613-622.

Ruland, J., & Mak, T. W. (2003). Transducing signals from antigen receptors to nuclear factor kappaB. *Immunol Rev, 193*, 93-100.

Sánchez, M., González-Burgos, E., Iglesias, I., & Gómez-Serranillos, M. P. (2020). Pharmacological update properties of *Aloe vera* and its major active constituents. *Molecules, 25*(6).

Saniasiaya, J., Salim, R., Mohamad, I., & Harun, A. (2017). Antifungal effect of

Malaysian *Aloe vera* leaf extract on selected fungal species of pathogenic otomycosis species in in vitro culture medium. *Oman Medical Journal, 32*, 41-46.

Sanyang, M. L., Sapuan, S., Jawaid, M., Ishak, M., & Sahari, J. (2015). Effect of plasticizer type and concentration on tensile, thermal and barrier properties of biodegradable films based on sugar palm (*Arenga pinnata*) starch. *Polymers, 7*, 1106-1124.

Senftleben, U., & Karin, M. (2002). The IKK/NF-kappa B pathway. *Crit Care Med, 30*(1 Suppl), S18-26.

Silva, S., Michniak-Kohn, B., & Leonardi, G. R. (2017). An overview about oxidation in clinical practice of skin aging. *An Bras Dermatol, 92*(3), 367-374.

Siti, M., Mohammad, S., Abd.Rahman, N., Sahaid, M., Khalil, S., Rozaimah, S., & Abdullah, S. (2014). An overview of biocellulose production using *Acetobacter xylinum* culture. *Biological research, 8*, 307-313.

Sjerobabski-Masnec, I., & Situm, M. (2010). Skin aging. *Acta Clin Croat, 49*(4), 515-518.

Südel, K. M., Venzke, K., Mielke, H., Breitenbach, U., Mundt, C., Jaspers, S., . . . Gallinat, S. (2005). Novel aspects of intrinsic and extrinsic aging of human skin: beneficial effects of soy extract. *Photochem Photobiol, 81*(3), 581-587.

Suksaeree, J., Monton, C., Charoenchai, L., & Pathompak, P. (2014). Preparation and evaluation of rice bran oil mask. *International Journal of Pharmacy and Pharmaceutical Sciences, 6*, 530-533.

Sun, Y. N., Li, W., Lee, S. H., Jang, H. D., Ma, J. Y., & Kim, Y. H. (2017). Antioxidant and anti-osteoporotic effects of anthraquinones and related constituents from the aqueous dissolved Aloe exudates. *Nat Prod Res, 31*(23), 2810-2813.

Surjushe, A., Vasani, R., & Saple, D. G. (2008). Aloe vera: a short review. *Indian J Dermatol, 53*(4), 163-166.

Teplicki, E., Ma, Q., Castillo, D. E., Zarei, M., Hustad, A. P., Chen, J., & Li, J. (2018). The effects of aloe vera on wound healing in cell proliferation, migration, and viability. *Wounds, 30*(9), 263-268.

Thanakkasaranee, S., Jantanasakulwong, K., Phimolsiripol, Y., Leksawasdi, N.,

Seesuriyachan, P., Chaiyaso, T., . . . Rachtanapun, P. (2021). High substitution synthesis of carboxymethyl chitosan for properties improvement of carboxymethyl chitosan films depending on particle sizes. *Molecules, 26*(19), 6013.

Xiang, H., Cao, F., Ming, D., Zheng, Y., Dong, X., Zhong, X., . . . Wang, D. (2017). Aloe-emodin inhibits Staphylococcus aureus biofilms and extracellular protein production at the initial adhesion stage of biofilm development. *Appl Microbiol Biotechnol, 101*(17), 6671-6681.

Xu, L., Chan, C. O., Lau, C. C., Yu, Z., Mok, D. K., & Chen, S. (2012). Simultaneous determination of eight anthraquinones in semen cassiae by HPLC-DAD. *Phytochemical Analysis, 23*(2), 110-116.

Yousef, H., Alhajj, M., & Sharma, S. (2021). Anatomy, skin (integument), epidermis *StatPearls*. Treasure Island (FL): StatPearls Publishing.

Zhao, F., Chen, L., Bi, C., Zhang, M., Jiao, W., & Yao, X. (2013). In vitro anti-inflammatory effect of picrasmalignan A by the inhibition of iNOS and COX-2 expression in LPS-activated macrophage RAW 264.7 cells. *Molecular Medicine Reports, 8*(5), 1575-1579.

APPENDIX

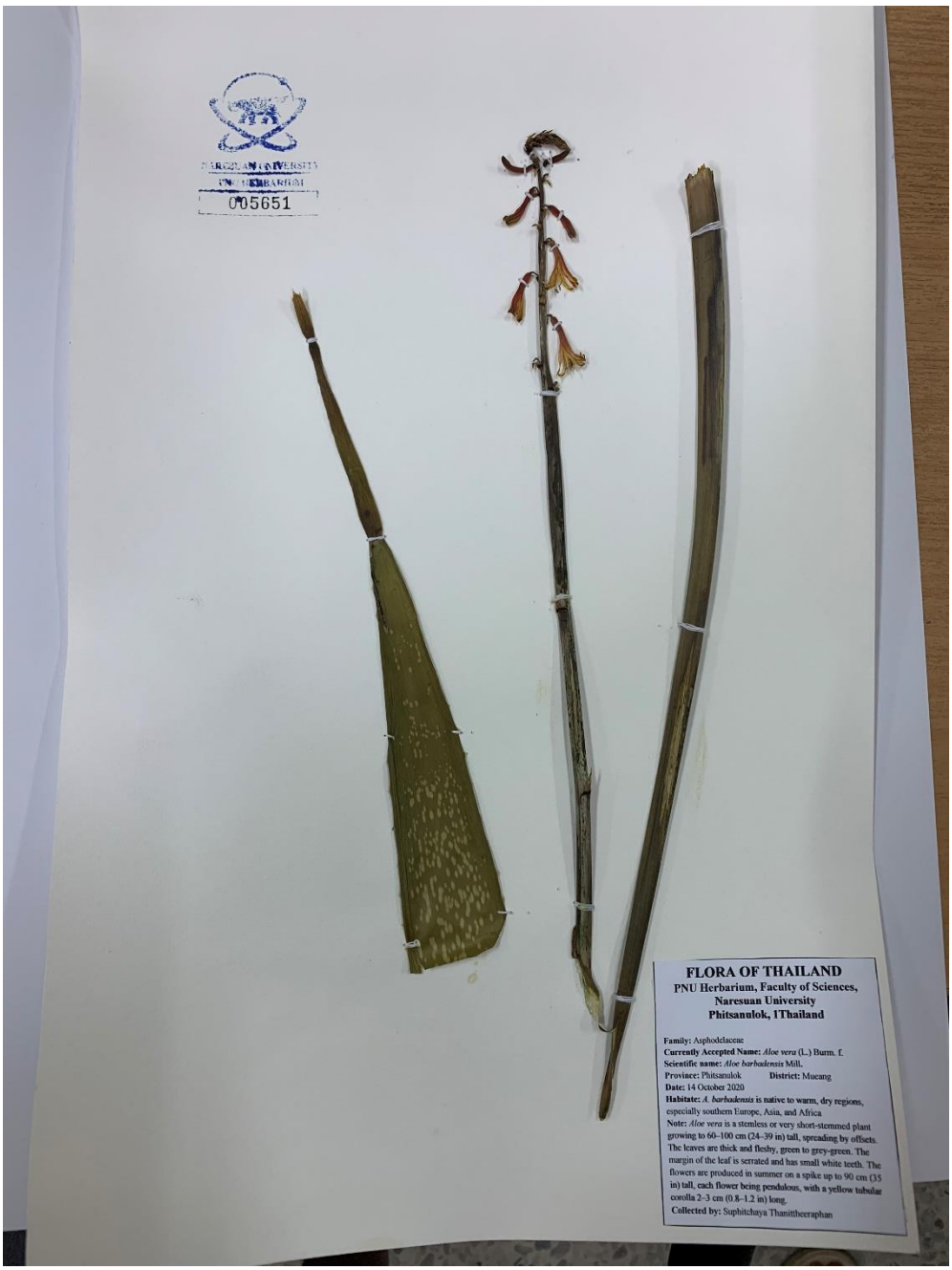

Figure 24 The voucher herbarium specimen of *Aloe vera*

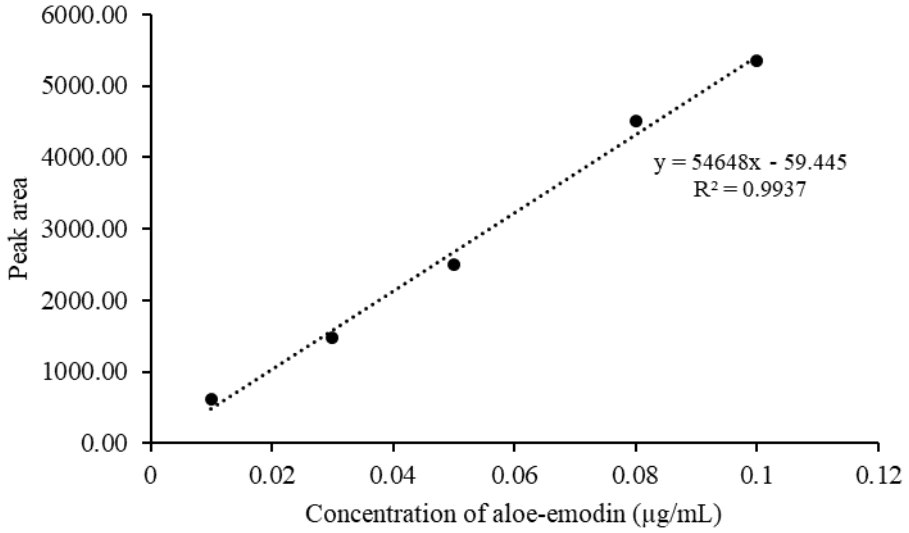

Figure 25 Calibration curve of aloe-emodin standard

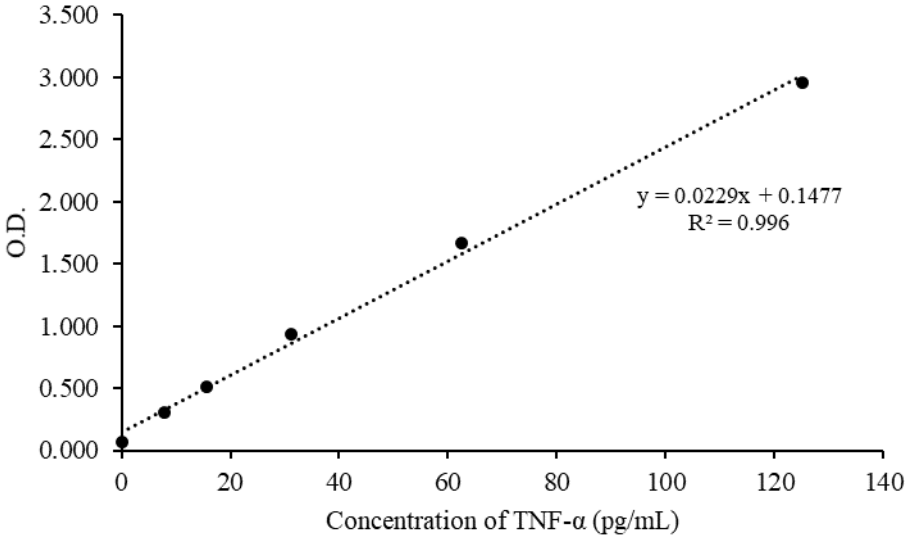

Figure 26 Calibration curve of TNF-α standard

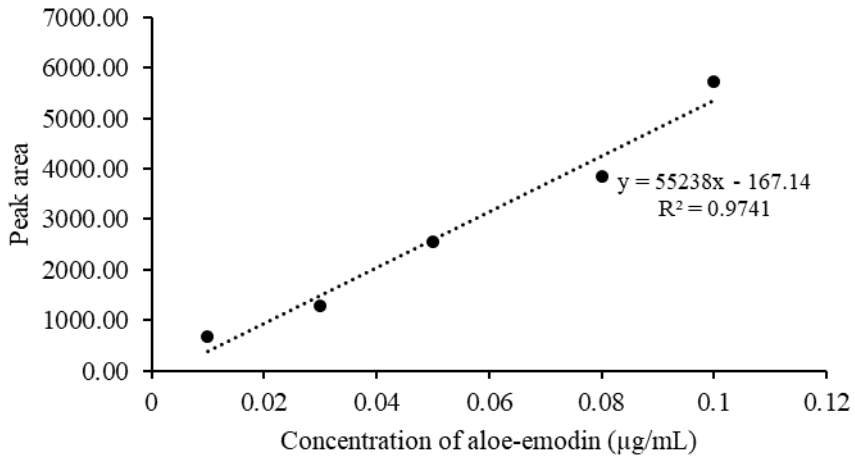

Figure 27 Calibration curve of aloe-emodin standard in release study

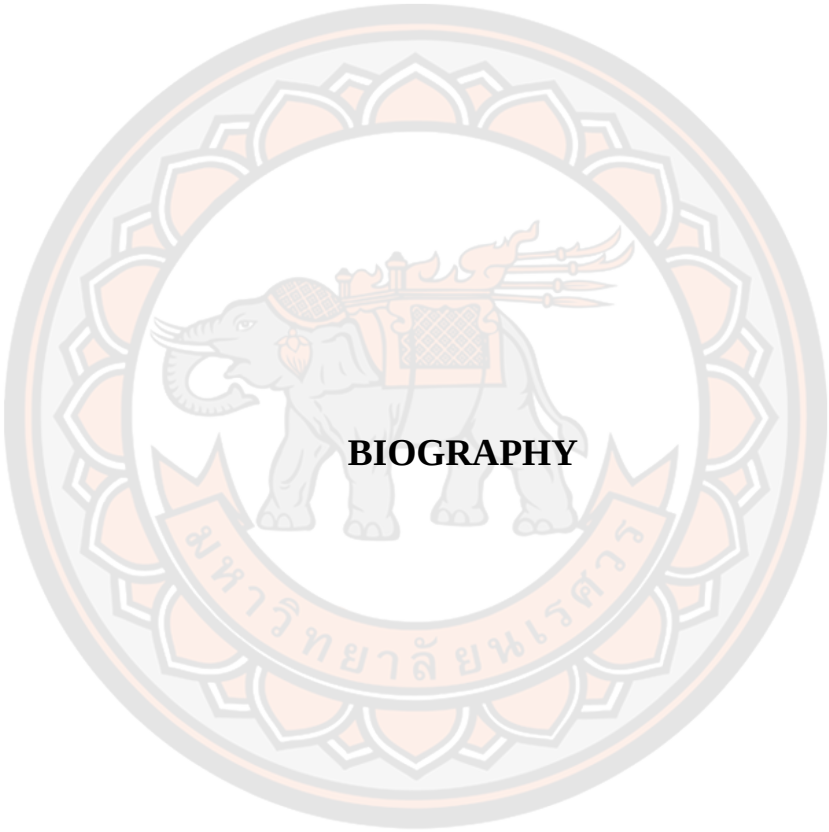

BIOGRAPHY

BIOGRAPHY

Name-Surname Suphitchaya Thanittheeraphan

Date of Birth

Address

Education Background 2016 B.S. (Cosmetic Sciences) Naresuan University